

REPORT NO.  
UCB/EERC-88/18  
NOVEMBER 1988

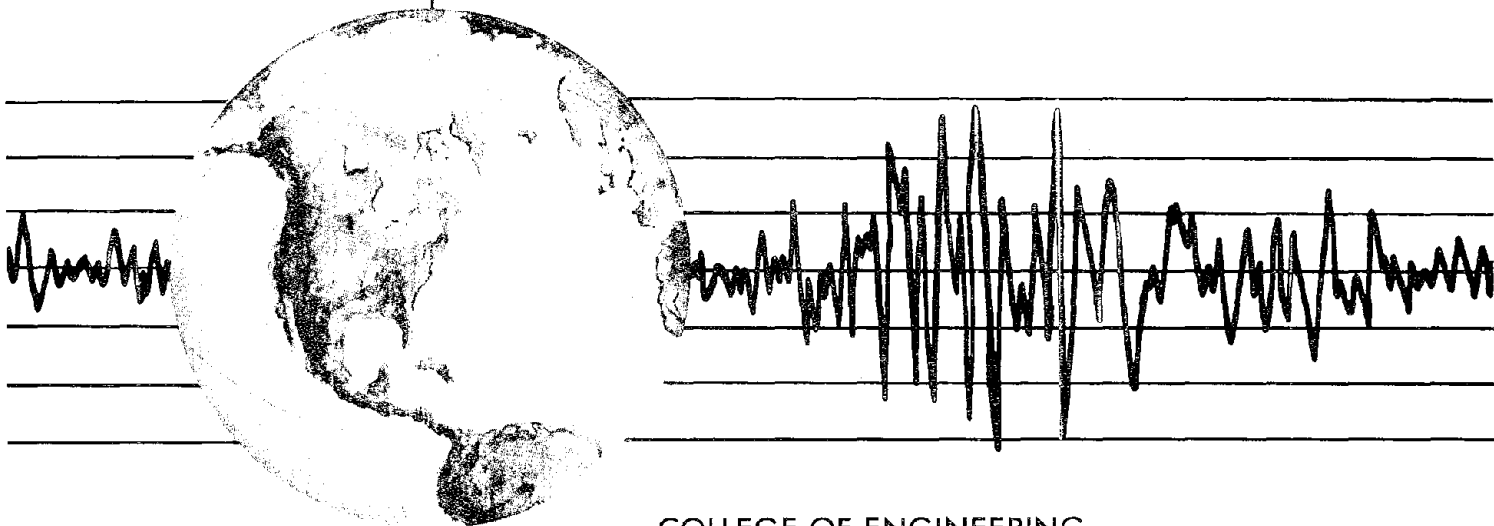
EARTHQUAKE ENGINEERING RESEARCH CENTER

# USE OF ENERGY AS A DESIGN CRITERION IN EARTHQUAKE-RESISTANT DESIGN

by

CHIA-MING UANG  
VITELMO V. BERTERO

Report to the National Science Foundation



COLLEGE OF ENGINEERING  
UNIVERSITY OF CALIFORNIA AT BERKELEY



<b>REPORT DOCUMENTATION PAGE</b>		<b>1. REPORT NO.</b> NSF/ENG-88053	<b>2.</b>	<b>3.</b> PB91-210906
<b>4. Title and Subtitle</b> "Use of Energy as a Design Criterion in Earthquake-Resistant Design."			<b>5. Report Date</b> November 1988	
<b>7. Author(s)</b> Chia-Ming Uang, V. V. Bertero			<b>8. Performing Organization Rept. No.</b> UCB/EERC-88/18	
<b>9. Performing Organization Name and Address</b> Earthquake Engineering Research Center University of California 1301 S 46th St. Richmond, CA 94804			<b>10. Project/Task/Work Unit No.</b>	
<b>12. Sponsoring Organization Name and Address</b> National Science Foundation 1800 G. St. NW Washington, DC 20550			<b>11. Contract(C) or Grant(G) No.</b> CES-8810563 (G) CES-88004305 ECE-8610870	
<b>15. Supplementary Notes</b>			<b>13. Type of Report &amp; Period Covered</b>	
<b>16. Abstract (Limit: 200 words)</b> The conventional derivation of an energy equation for the seismic response of structures is reviewed and compared with an alternative definition which is physically more meaningful. The following engineering parameters computed using these two definitions are compared: (1) the profiles of energy time histories for short and long period structures, which are shown to be significantly different; (2) input energy spectra based on a constant ductility ratio for which significant differences exist for both the short and long period ranges, although for periods in the range of practical interest in building design the difference is small for most of the recorded ground motions. It was also found that the maximum input energy is closely correlated to the strong motion duration.  The reliability of using input energy spectra derived for a single-degree-of-freedom system to predict the input energy to multi-story buildings is illustrated by correlating the analytical prediction with the experimental results of a six-story steel frame. Finally, the uniqueness of the energy dissipation capacity of a structural member is evaluated. Test results for three types of structural members--steel beams, reinforced concrete shear walls, and composite beams--are examined, with the conclusion that the energy dissipation capacity is not unique but is highly dependent on the loading and deformation paths.			<b>14.</b>	
<b>17. Document Analysis a. Descriptors</b> energy seismic response of structures ductility ratio input energy energy dissipation capacity <b>b. Identifiers/Open-Ended Terms</b> steel beams shear walls composite beams  <b>c. COSATI Field/Group</b>				
<b>18. Availability Statement:</b> release unlimited			<b>19. Security Class (This Report)</b> unclassified	
			<b>21. No. of Pages</b> 57	
			<b>20. Security Class (This Page)</b> unclassified	
			<b>22. Price</b>	



*i-a.*

# **USE OF ENERGY AS A DESIGN CRITERION IN EARTHQUAKE-RESISTANT DESIGN**

*Chia-Ming Uang*

Assistant Professor  
Department of Civil Engineering  
Northeastern University  
360 Huntington Avenue  
Boston, MA 02115

*Vitelmo V. Bertero*

Professor  
Department of Civil Engineering  
University of California, Berkeley  
Berkeley, CA 94720

**Report No. UCB/EERC-88/18**  
**Earthquake Engineering Research Center**  
**College of Engineering**  
**University of California**  
**Berkeley, California**

**November 1988**



## ABSTRACT

The conventional derivation of an energy equation for the seismic response of structures is reviewed and compared with an alternative definition which is physically more meaningful. The following engineering parameters computed using these two definitions are compared: (1) the profiles of energy time histories for short and long period structures, which are shown to be significantly different; (2) input energy spectra based on a constant ductility ratio for which significant difference exists for both the short and long period ranges, although for periods in the range of practical interest in building design the difference is small for most of the recorded ground motions. It was also found that the maximum input energy is closely correlated to the strong motion duration.

The reliability of using input energy spectra derived for a single-degree-of-freedom system to predict the input energy to multi-story buildings is illustrated by correlating the analytical prediction with the experimental results of a six-story steel frame. Finally, the uniqueness of the energy dissipation capacity of a structural member is evaluated. Test results for three types of structural members — steel beams, reinforced concrete shear walls, and composite beams — are examined, with the conclusion that the energy dissipation capacity is not unique but is highly dependent on the loading and the deformation paths.





## **ACKNOWLEDGEMENTS**

This research is sponsored by the National Science Foundation, Grant No. CES-8810563 to the first author and Grants No. CES-8804305 and No. ECE-8610870 to the second author. Any opinions, discussions, findings, conclusions, and recommendations are those of the authors and do not necessarily reflect the views of the sponsor.

Dr. M. J. Huang of the Division of Mines and Geology, California Department of Conservation provided the processed records of the 1986 San Salvador Earthquake. Dr. Beverley Bolt and Dr. Andrew S. Whittaker reviewed this report. Their contributions to this research are gratefully acknowledged.

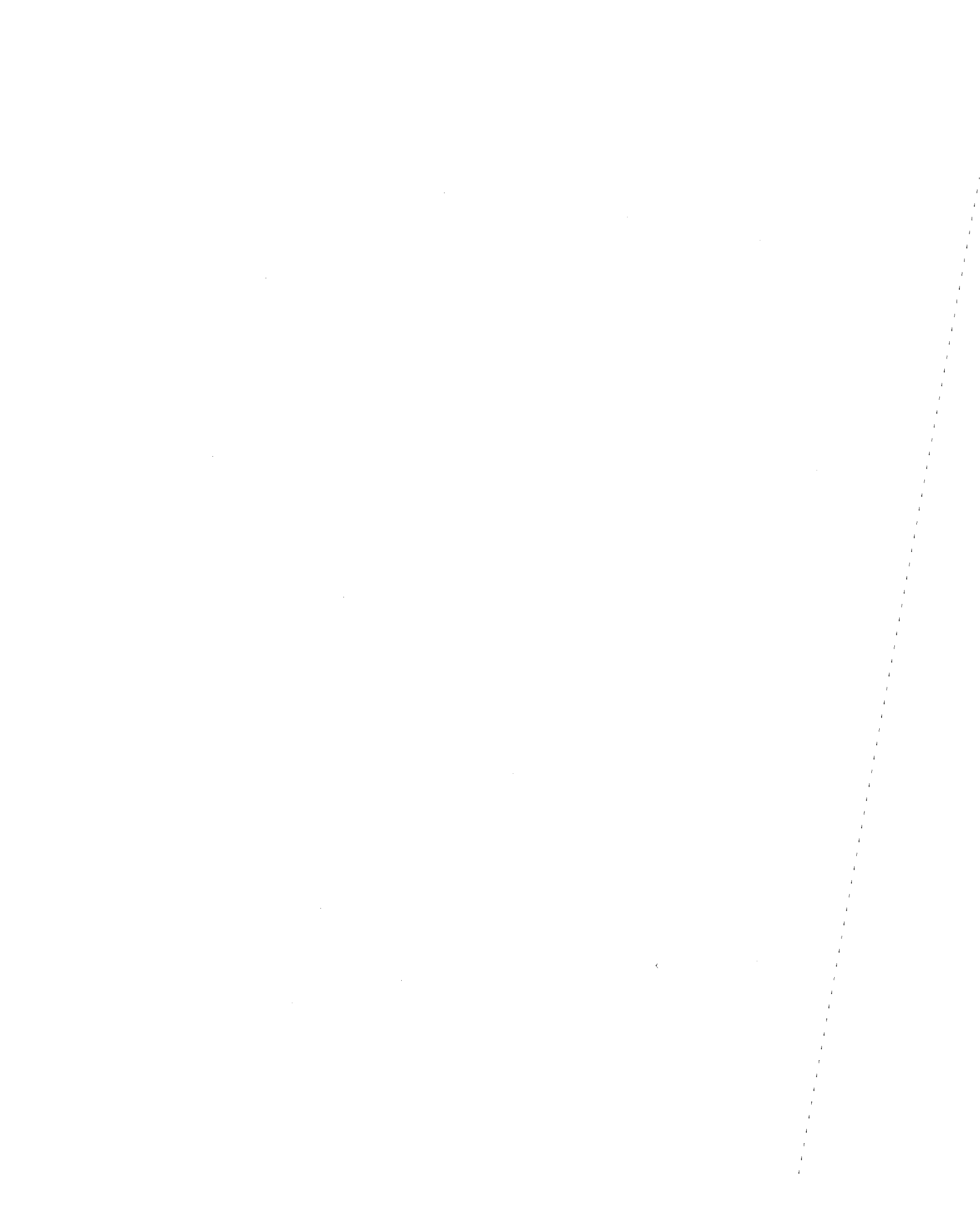


## TABLE OF CONTENTS

ABSTRACT .....	i
ACKNOWLEDGEMENTS .....	ii
TABLE OF CONTENTS .....	iii
LIST OF TABLES .....	v
LIST OF FIGURES .....	vi
I. INTRODUCTION .....	1
1.1 Statement of the Problem .....	1
1.2 Objectives .....	1
1.3 Scope .....	2
II. PREDICTION OF INPUT ENERGY DEMANDS .....	3
2.1 Derivation of Energy Equations for a SDOF System .....	3
2.1.1 Method 1 - Derivation of “Absolute” Energy Equation .....	4
2.1.2 Method 2 - Derivation of “Relative” Energy Equation .....	5
2.2 Comparison of Energy Time Histories .....	5
2.3 Estimation of the Difference between Input Energies from Different Definitions .....	6
2.4 Comparison of Input Energy Spectra .....	8
2.5 Influence of Displacement Ductility Ratios on Input Energy Spectra .....	9
2.6 Verification of Housner’s Assumption .....	10
2.7 Approximate Inelastic Input Energy Spectra .....	10
2.8 Input Energy Equivalent Velocity Amplification Factor and Strong Motion Duration Relationship .....	11
2.9 Input Energy to Multi-Story Buildings .....	13



III. ESTIMATION OF STRUCTURAL MEMBER ENERGY SUPPLY .....	15
3.1 Introductory Remarks .....	15
3.2 Steel Beam Testing .....	15
3.3 Shear Wall Testing .....	16
3.4 Composite Beam Testing .....	16
3.5 Concluding Remarks .....	17
IV. CONCLUSIONS .....	18
REFERENCES .....	20
NOTATION .....	23
TABLE .....	25
FIGURES .....	26



## LIST OF TABLES

Table 1.1 Earthquake Record Data





## LIST OF FIGURES

- Fig. 1.1 Earthquake Ground Motion Acceleration Time Histories
- Fig. 2.1 Mathematical Model of a SDOF System subjected to an Earthquake Ground Motion
- Fig. 2.2 Energy Time Histories for an Elastic-Perfectly Plastic System subjected to the 1971 San Fernando Earthquake — Pacoima Dam Record (Ductility Ratio 3, 5% Damping)
- Fig. 2.3 Comparison of Input Energy Equivalent Velocity Spectra for Ductility Ratio 5 (5% Damping)
- Fig. 2.4 Comparison of Absolute Input Energy Equivalent Velocity Spectra for Ductility Ratios 2, 5, and 8 (5% Damping)
- Fig. 2.5 Comparison of Absolute Input Energy Equivalent Velocity Spectra and Linear Elastic Pseudo-velocity Response Spectra for Ductility Ratio 5 (5% Damping for  $V_i$  and  $S_{pv}$ )
- Fig. 2.6 Comparison of Absolute Input Energy and Iwan's Elastic Input Energy Equivalent Velocity Spectra for Ductility Ratio 5 (5% Damping)
- Fig. 2.7 Input Energy Equivalent Velocity Amplification Factor and Strong Motion Duration Relationship
- Fig. 2.8 Overall View of 0.3-Scale Model with Reference Frame
- Fig. 2.9 Envelope of Critical Inter-story Drift Index versus Base Shear Ratio
- Fig. 2.10 Model Collapse Level Test (MO-65 Test) Energy Time Histories
- Fig. 2.11 Comparison of Analytical and Experimental Input Energy Equivalent Velocities (Measured Ground Motion during MO-65 Test, 2% Damping Ratio)
- Fig. 3.1 Number of Cycles Required to Attain Fracture as a Function of the Controlling Strain
- Fig. 3.2 Idealized Steel Beam Moment-Curvature Relationship
- Fig. 3.3 Comparison of Energy Dissipation Capacities of Two Shear Walls (Wall 1: Cyclic Loading; Wall 3: Monotonic Loading)
- Fig. 3.4 Comparison of Energy Dissipation Capacities of Two Composite Girders



## I. INTRODUCTION

### 1.1. Statement of the Problem

Traditionally, displacement ductility has been used as a criterion to establish inelastic design response spectra (IDRS) for earthquake-resistant design of buildings.<sup>16,21</sup> The minimum required *strength* (or capacity for lateral force) of a building is then based on the selected IDRS. As an alternative to this traditional design approach, an energy-based method was proposed by Housner.<sup>10</sup> Although Anderson and Bertero<sup>3</sup> estimated the energy input in steel structures designed considering inelastic behavior in 1969, it is only recently that this approach has gained extensive attention.<sup>2,5,8,12-15,18,22</sup> This design method is based on the premise that the *energy demand* during an earthquake (or an ensemble of earthquakes) can be predicted and that the *energy supply* of a structural element (or a structural system) can be established. A satisfactory design implies that the energy supply should be larger than the energy demand.

### 1.2. Objectives

The first objective of this report is to analyze the physical meaning of two energy equations that are derived and used in the literature. The second objective is to use these two definitions to construct inelastic input energy spectra for a single-degree-of-freedom (SDOF) system, and then to compare the spectra, as well as to evaluate the reliability of using SDOF energy spectra to predict the input energy to multi-story buildings. The third objective is to assess the reliability of predicting the energy dissipation capacity of a given structural member or structural system, and to investigate how different loading and deformation paths can affect the energy dissipation capacities of structural members.

### **1.3. Scope**

Evaluation of the energy equations is limited to an elastic-perfectly plastic SDOF system. Five earthquake ground motions (see Table 1.1 and Fig. 1.1) including some recently recorded destructive earthquakes are used in this study. The reliability of using SDOF input energy spectra for determining the input energy to a multi-story building is assessed by studying the correlation of SDOF results with those obtained from shaking table experiments conducted on a six-story steel frame. The energy supplies, in particular energy dissipation capacities, of three types of structural members — steel, reinforced concrete and composite members — subjected to cyclic loading, are discussed.

## II. PREDICTION OF INPUT ENERGY DEMANDS

### 2.1. Derivation of Energy Equations for a SDOF System

Given a viscous damped SDOF system subjected to a horizontal earthquake ground motion (Fig. 2.1a), the equation of motion can be written as

$$m\ddot{v}_t + c\dot{v} + f_s = 0 \quad (2.1)$$

where  $m$  = mass

$c$  = viscous damping coefficient

$f_s$  = restoring force

$v_t = v + v_g$  = absolute (or total) displacement of the mass

$v$  = relative displacement of the mass with respect to the ground

$v_g$  = earthquake ground displacement.

Note that  $f_s$  may be expressed as  $kv$  for a linear elastic system ( $k$  = stiffness.) By letting  $\ddot{v}_t = \ddot{v} + \ddot{v}_g$ , Eq. 2.1 may be rewritten as

$$m\ddot{v} + c\dot{v} + f_s = -m\ddot{v}_g \quad (2.2)$$

Therefore the structural system in Fig. 2.1a can be conveniently treated as the equivalent system in Fig. 2.1b with a fixed base and subjected to an effective horizontal dynamic force of magnitude  $-m\ddot{v}_g$ . Although both systems give the same relative displacement, this "convenience" does cause some confusion in the definition of input energy and kinetic energy. Depending upon whether Eq. 2.1 or 2.2 is used to derive the energy equation, different definitions of input and kinetic energies may result.

### 2.1.1. Method 1 — Derivation of “Absolute” Energy Equation

Integrate Eq. 2.1 with respect to  $v$  from the time that the ground motion excitation starts:

$$\int m\ddot{v}_t dv + \int c\dot{v}dv + \int f_s dv = 0 . \quad (2.3)$$

Replacing  $v$  by  $(v_t - v_g)$  in the first term in Eq. 2.3, then

$$\int m\ddot{v}_t dv = \int m\ddot{v}_t (dv_t - dv_g) = \int m \frac{d\dot{v}_t}{dt} dv_t - \int m\ddot{v}_t dv_g = \frac{m(\dot{v}_t)^2}{2} - \int m\ddot{v}_t dv_g . \quad (2.4)$$

Substituting Eq. 2.4 into Eq. 2.3 yields

$$\frac{m(\dot{v}_t)^2}{2} + \int c\dot{v}dv + \int f_s dv = \int m\ddot{v}_t dv_g . \quad (2.5)$$

The first term of the above equation is the “absolute” kinetic energy  $E_k$

$$E_k = \frac{m(\dot{v}_t)^2}{2} \quad (2.6)$$

because *absolute* velocity ( $\dot{v}_t$ ) is used to calculate the kinetic energy. The second term in Eq. 2.5 is the damping energy ( $E_\xi$ ), which is always non-negative because

$$E_\xi = \int c\dot{v}dv = \int c\dot{v}^2 dt . \quad (2.7)$$

The third term in Eq. 2.5 is the absorbed energy ( $E_a$ ), which is composed of recoverable elastic strain energy ( $E_s$ ) and irrecoverable hysteretic energy ( $E_h$ ):

$$E_a = \int f_s dv = E_s + E_h \quad (2.8)$$

where  $E_s = \frac{(f_s)^2}{2k}$ .

The right-hand side term in Eq. 2.5 is, by definition, the input energy ( $E_i$ ):

$$E_i = \int m\ddot{v}_t dv_g . \quad (2.9)$$

In this study  $E_i$  is defined as the “absolute” input energy. This definition is physically meaningful in that the term  $m\ddot{v}_t$  represents the inertia force applied to the structure. This force, which from Eq. 2.1 is equal to restoring force plus damping force, is the same as the total force applied to the structure foundation. Therefore  $E_i$  represents the work done by the total base shear at the foundation on the foundation displacement. The absolute energy equation (Eq. 2.5) then can be

written as follows:

$$E_i = E_k + E_\xi + E_a = E_k + E_\xi + E_s + E_h . \quad (2.10)$$

### 2.1.2. Method 2 — Derivation of “Relative” Energy Equation

Integrate Eq. 2.2 with respect to  $v$ :

$$\int m\dot{v}dv + \int c\dot{v}dv + \int f_s dv = -\int m\ddot{v}_g dv . \quad (2.11)$$

Notice that the second term ( $=E_\xi$ ) and the third term ( $=E_a$ ) on the left side of the equation remain unchanged. The first term in Eq. 2.11 can be rewritten as

$$\int m\dot{v}dv = \int m \frac{d\dot{v}}{dt} dv = \int m d\dot{v}(\dot{v}) = \frac{m(\dot{v})^2}{2}$$

which is the “relative” kinetic energy ( $E'_k$ ) calculated from relative velocity:

$$E'_k = \frac{m(\dot{v})^2}{2} . \quad (2.12)$$

The right-hand side term of Eq. 2.11 is conventionally defined as the “input energy” ( $E'_i$ ):

$$E'_i = -\int m\ddot{v}_g dv . \quad (2.13)$$

In this study  $E'_i$  is defined as the “relative” input energy. This definition of input energy physically represents the work done by the static equivalent lateral force ( $-m\ddot{v}_g$ ) on the equivalent fixed-base system; that is, it neglects the effect of the rigid body translation of the structure. The relative energy equation is then expressed as

$$E'_i = E'_k + E_\xi + E_a = E'_k + E_\xi + E_s + E_h . \quad (2.14)$$

## 2.2. Comparison of Energy Time Histories

Input energy as defined by either Eq. 2.9 or 2.13 is a function of time. Figure 2.2 shows the energy time histories for a short period ( $T = 0.2$  sec) and a long period ( $T = 10.0$  sec) elastic-perfectly plastic SDOF structure subjected to the 1971 Pacoima Dam earthquake ground motion.

Damping energy ( $E_\xi$ ), strain energy ( $E_s$ ), and hysteretic energy ( $E_h$ ) terms are uniquely defined, irrespective of what method is used, but the input energy and kinetic energy are different,

depending upon which method is used. High fluctuations in the  $E_i$  time history are apparent for the short period structure, and the same phenomenon for  $E'_i$  is apparent for the long period structure. Note also the significant difference in the magnitudes of  $E_i$  and  $E'_i$  for the long period structure. When the period of the structure is significantly larger than the predominant excitation period of the ground motion, the structure's center-of-mass essentially remains stationary. Therefore the absolute input energy for the relatively long period structure should be low, as is reflected in the  $E_i$  time history.

To construct input energy spectra, the time at which the input energy is evaluated should be specified. Most previous researchers evaluated the input energy at either (i) the end of the earthquake ground motion, or at (ii) the end of the earthquake ground motion plus a time equal to one half of the period of free vibration of the structure,<sup>22</sup> or at (iii) the end of the earthquake ground motion plus a time at which the velocity of the structure changes sign.<sup>12</sup> If the relative energy equation is used, the time at which the input energy is evaluated by the methods just described, is suitable for short period structures (see Fig. 2.2); for long period structures these methods may significantly underestimate the maximum input energy that may occur early in the ground motion (see Fig. 2.2b.) For this reason the maximum input energy measured during the ground motion is used to construct the input energy spectra in this study. It should be noted that if  $E_i$  and  $E'_i$  are evaluated at the end of the ground motion, which corresponds to the time at which  $\dot{v}_g = 0$ , the rigid body kinetic energy is zero and hence the values of  $E_i$  and  $E'_i$  are identical.

To solve the problem of the nonzero initial condition of each ground motion, the method of prefixing a two second acceleration pulse, proposed by Pecknold and Riddle,<sup>17</sup> was adopted in these analyses.

### 2.3. Estimation of the Difference between Input Energies from Different Definitions

The definition of input energy given by Eq. 2.9 has been used by Berg and Thomaidis,<sup>5</sup> Goel and Berg,<sup>8</sup> Mahin and Lin,<sup>14</sup> Uang and Bertero,<sup>20</sup> among others. Equation 2.13 has been used by most other researchers. The difference between the input energies of Methods 1 and 2 is derived below.



$$\begin{aligned}
 E_i &= \int (m\ddot{v}_t)dv_g = \int (m\ddot{v}_t)(dv_t - dv) = \int (m\ddot{v}_t)dv_t - \int m(\ddot{v} + \ddot{v}_g)dv \\
 &= \frac{m}{2}(\dot{v}_t)^2 - \frac{m}{2}(\dot{v})^2 + E'_i = \frac{m}{2}(\dot{v}_g)^2 + m\dot{v}\dot{v}_g + E'_i
 \end{aligned}$$

that is,

$$E_i - E'_i = \frac{m}{2}(\dot{v}_g)^2 + m\dot{v}\dot{v}_g . \quad (2.15a)$$

It can be proved easily that the difference between the kinetic energies due to the different definitions is:

$$E_k - E'_k = \frac{m}{2}(\dot{v}_g)^2 + m\dot{v}\dot{v}_g . \quad (2.15b)$$

Because the last term in the above equation contains the term  $\dot{v}$ , the error cannot be estimated easily. However, the values of  $E_i$  and  $E'_i$  for very long and very short period structures can be calculated as follows.

**For a structure with very long period ( $T \rightarrow \infty$ ),** the input energy tends to converge to a constant value, depending upon which definition of input energy is used. For a structure with infinitely long period,

$$\begin{aligned}
 v &= -v_g \\
 v_t = v + v_g &= 0 \quad ; \quad \ddot{v}_t = 0 .
 \end{aligned}$$

Therefore,

$$\text{Method 1: } \frac{E_i}{m} = \int \ddot{v}_t dv_g = \int (0) dv_g = 0 \quad (2.16a)$$

$$\text{Method 2: } \frac{E'_i}{m} = -\int \ddot{v}_g dv = -\int \ddot{v}_g (-dv_g) = \int \ddot{v}_g dv_g = \frac{(\dot{v}_g)^2}{2} \quad (2.16b)$$

i.e., the difference between the input energies  $E_i$  and  $E'_i$  for a structure with  $T = \infty$  is equal to  $m(\dot{v}_g)^2/2$ . If the input energy  $E'_i$  is evaluated at the end of duration, its value will be very small because  $\dot{v}_g$  tends to be vanishingly small. If  $E'_i$  is evaluated as the maximum throughout the duration, then  $E'_i/m$  will then converge to  $\dot{v}_{g(max)}^2/2$  for long period structures.

**For a structure with very short period ( $T \rightarrow 0$ ),** the input energy will also converge to a constant value, depending upon the definition used. For a structure with zero period, i.e., a rigid

structure,

$$\ddot{v}_t = \ddot{v}_g$$

$$v_t = v_g, \quad \text{or } v = 0.$$

Therefore,

Method 1: 
$$\frac{E_i}{m} = \int \ddot{v}_t dv_g = \int \ddot{v}_g dv_g = \frac{(\dot{v}_g)^2}{2} \quad (2.17a)$$

Method 2: 
$$\frac{E'_i}{m} = -\int \ddot{v}_g dv = -\int \ddot{v}_g (0) = 0 \quad (2.17b)$$

i.e., the difference between the input energy spectra for a structure with zero period is equal to  $m\dot{v}_{g(max)}^2/2$ .

On the basis of the above derivation, it appears that from the energy point of view the peak ground velocity plays an important role as a damage index. It would be misleading, however, to use  $E_i$  as a damage index for very long period structures because the value of  $E_i$  is very small. Such structures are so flexible that nonstructural component damage in real buildings may be excessive. The use of  $E'_i$  in this case may give a more reasonable index for damage. Similarly, the use of  $E_i$  for a very short period structure serves as a better damage index than the use of  $E'_i$ . Relative input energy may give misleading information for a rigid structure because Eq. 2.17b implies that no energy is input to a rigid structure.

#### 2.4. Comparison of Input Energy Spectra

The input energy spectra for five earthquake records (see Table 1.1) are generated for a constant displacement ductility of five. The input energy is converted to an equivalent velocity by the following relationship:

$$V_i = \sqrt{\frac{2E_i}{m}} \quad ; \quad V'_i = \sqrt{\frac{2E'_i}{m}} \quad (2.18)$$

The input energy equivalent velocity spectra are shown in Fig. 2.3; the solid line represents the input energy calculated by Method 1 and the dashed line by Method 2. Note again that the input energy ( $E_i$  or  $E'_i$ ) plotted is the maximum input energy; this energy may occur before the ground motion ends.

Figure 2.3 shows that  $V_i$  and  $V'_i$  are very close in the intermediate period ranges: to be more specific, the input energies calculated by Methods 1 or 2 are very close in the vicinity of the predominant excitation periods of the earthquake ground motions. The difference between  $V_i$  and  $V'_i$  increases for longer and shorter period structures. The level of maximum ground velocity  $\dot{v}_{g(max)}$  is also shown in Fig. 2.3 for each earthquake record. The trend that  $V_i$  converges to  $\dot{v}_{g(max)}$  as the period of the structure tends to zero and that  $V'_i$  converges to  $\dot{v}_{g(max)}$  as the period of the structure tends to infinity (as stated in Eqs. 2.16b and 2.17a) is clearly shown in Fig. 2.3. The tendency for  $V'_i$  in the short period range and for  $V_i$  in the long period range to decrease to zero can also be observed (see Eqs. 2.16a and 2.17b.)

## 2.5. Influence of Displacement Ductility Ratios on Input Energy Spectra

It has been concluded that  $E'_i$  (or  $V'_i$  in the form of equivalent velocity) spectral values evaluated at the end of the duration of the ground motion are relatively insensitive to the displacement ductility level.<sup>22</sup> The variation of input energy equivalent velocity spectra for displacement ductility ratios of 2, 5, and 8 are shown in Fig. 2.4. It can be observed that the input energy ( $E_i$ ) spectra are generally insensitive to the level of ductility ratio. The only exceptions to this observation are the spectra of the 1985 Mexico City Earthquake. For this highly harmonic, long duration earthquake record the input energy is significantly affected by the ductility level (especially from  $\mu = 2$  to  $\mu = 5$ ) in the period range to the left side of the predominant excitation period.

The peak of the spectrum, which corresponds to the predominant period of the ground motion, tends to shift slightly towards a smaller period value as the displacement ductility ratio is increased. Therefore, as the value of the displacement ductility ratio increases, the values of  $V_i$  in the period range immediately to the left of the peak increase and the values in the period range to the right of the peak decrease.

## 2.6. Verification of Housner's Assumption

For a linear elastic system the maximum input energy that is *stored* in a SDOF system is

$$E_D = \frac{1}{2} k (S_d)^2 = \frac{1}{2} m (S_{pv})^2 \quad (2.19)$$

where  $S_d$  is the linear elastic spectral displacement and  $S_{pv}$  is the linear elastic pseudo-velocity, both being a function of period and damping ratio. It should be noted that  $E_D$  is the maximum elastic energy that is stored in the structure; the damping energy is not included. Housner<sup>10</sup> assumed that  $E_D$  (or  $S_{pv}$  in the form of equivalent velocity) can be used as the energy demand for an inelastic system in his proposed limit design method. If  $S_{pv}$  spectra with 5% damping are compared with the  $V_i$  spectra with 5% damping and a ductility ratio of 5, it is seen from Fig. 2.5 that  $S_{pv}$  may significantly underestimate  $V_i$ .

## 2.7. Approximate Inelastic Input Energy Spectra

Inelastic behavior has the effect of (i) increasing the effective natural period, and (ii) increasing the effective damping ratio of a structure. On the basis of a study of a class of hysteretic structures subjected to a total of 12 earthquake ground motions, Iwan<sup>11</sup> found that an inelastic response spectrum can be approximated by an elastic spectrum corresponding to an equivalent viscous damping ( $\xi_e$ ) and an equivalent natural period ( $T_e$ ):

$$\xi_e = \xi + 0.0587 (\mu-1)^{0.371} \quad (2.20a)$$

$$\frac{T_e}{T} = 1 + 0.121 (\mu-1)^{0.939} \quad (2.20b)$$

where  $\xi$  is the nominal viscous damping ratio,  $T$  is the natural period in the elastic range, and  $\mu$  is the ductility ratio.

For a given ductility ratio, the elastic input energy equivalent velocity spectra, constructed by using an equivalent damping ratio of  $\xi_e$  (Eq. 2.20a) and then performing a period shift using Eq. 2.20b, are compared with the inelastic spectra shown in Fig. 2.4. Figure 2.6 shows such a comparison for  $\mu = 5$ . It can be observed that although inelastic input energy equivalent velocity spectra appear to be predicted very well by elastic spectra constructed using Iwan's procedure, there are some significant differences. For example, for a period of about 2 seconds Iwan's

elastic  $V_i$  spectral value for the Mexico City earthquake is twice the inelastic  $V_i$  spectral value; and therefore the elastic  $E_i$  value will be 4 times the value of the inelastic  $E_i$ . It is believed that this can be attributed to the highly harmonic nature of the Mexico City ground motion and that this type of motion was not taken into account in Iwan's derivation of Eq. 2.20.

In his study of the relationship of  $\xi_e$  and  $T_e$  for both harmonic and typical earthquake excitations, Hadjian<sup>9</sup> has shown that the equivalent damping ratios due to harmonic excitation are about five times those due to earthquake excitation, and the period changes due to harmonic excitation are about twice those due to earthquake excitation. It is believed that Eq. 2.20 significantly underestimates the values of  $\xi_e$  and  $T_e$  for the 1985 Mexico City earthquake. An increase in the value of  $\xi_e$  will lower the magnitude of Iwan's elastic input energy spectra, making them more comparable to the actual inelastic input energy spectra. Deriving appropriate values of  $\xi_e$  and  $T_e$  for the 1985 Mexico City earthquake is outside the scope of this study.

## 2.8. Input Energy Equivalent Velocity Amplification Factor and Strong Motion Duration Relationship

It is well-known that elastic spectral values like elastic pseudo-acceleration cannot reflect the effect of strong motion duration. This shortcoming carries through to any inelastic design spectra derived from them. Since input energy reflects the effect of the duration directly through integration, it is worthwhile to investigate the relationship between the maximum equivalent velocity of input energy and the strong motion duration. Two quantities — amplification factor and the strong motion duration used in this study — are described first.

The amplification factor ( $\Psi$ ) of an input energy equivalent velocity spectrum for a given ductility ratio ( $\mu$ ) and a viscous damping ratio ( $\xi$ ) is defined by the following:

$$\Psi(\mu, \xi) = \frac{V_i^{\max}(\mu, \xi)}{\dot{v}_g(\max)} \quad (2.21)$$

where  $V_i^{\max}(\mu, \xi)$  is the maximum value of  $V_i$  evaluated throughout the whole period range. In general  $V_i^{\max}(\mu, \xi)$  occurs in the immediate vicinity of the predominant period of the earthquake ground motion.

One commonly used definition of strong motion duration is that due to Trifunac and Brady:<sup>19</sup>

$$t_D = t_{0.95} - t_{0.05} \quad (2.22)$$

where  $t_{0.05}$  and  $t_{0.95}$  define the times at which 5 percent and 95 percent, respectively, of the value of the Arias intensity ( $I_A$ ) is achieved. Arias intensity is defined as follows:<sup>4</sup>

$$I_A = \frac{\pi}{2g} \int_0^{t_d} \ddot{v}_g^2(t) dt \quad (2.23)$$

where  $t_d$  is the total duration of the earthquake record. The calculated values of  $t_D$  for each earthquake record are listed in Table 1.1. A plot of  $\Psi$  ( $\mu=5, \xi=5\%$ ) versus  $t_D$  for the five earthquake motions is shown in Fig. 2.7. It is observed that  $\Psi$  and  $t_D$  are linearly dependent; by letting the intercept of the line of best fit, shown in Fig. 2.7, be 1.0, the following equation is obtained by the method of least-squares:

$$\Psi (\mu=5, \xi = 5\%) = 1.0 + 0.12t_D \quad (2.24)$$

Therefore, if the strong motion duration at a given site is known, it is possible to predict the maximum energy input to a structure with a specified ductility ratio (5 for the case used in developing Eq. 2.24.) The period of the structure at which this maximum input energy occurs is close to the predominant excitation period of the expected earthquakes at the site under consideration.

For example, if it is expected from previous earthquake records at a certain site that the maximum ground velocity is 30 in/sec and that the strong motion duration  $t_D$  is 20 sec, the maximum input energy per unit mass for a structure having a damping ratio of 5 percent and a ductility ratio of 5 can be estimated by the following procedure:

$$\Psi = 1.0 + 0.12t_D = 1.0 + 0.12(20) = 3.4$$

$$V_i^{\max} = \Psi \dot{v}_g(\max) = 3.4(30) = 102 \text{ in/sec}$$

$$\frac{E_i^{\max}}{m} = \frac{1}{2}(V_i^{\max})^2 = \frac{1}{2}(102)^2 = 5,202 \text{ in}^2/\text{sec}^2 = 36 \text{ ft}^2/\text{sec}^2$$

## 2.9. Input Energy to Multi-Story Buildings

The “absolute” energy equation for an  $N$ -story building has been derived as follows:<sup>20</sup>

$$\frac{1}{2} \dot{\mathbf{v}}_t^T \mathbf{m} \dot{\mathbf{v}}_t + \int \dot{\mathbf{v}}_t^T \mathbf{c} d\mathbf{v} + \int \mathbf{f}_s^T d\mathbf{v} = \int \left( \sum_{i=1}^N m_i \ddot{v}_{ii} \right) dv_g \quad (2.25)$$

where  $\mathbf{m}$ ,  $\mathbf{c}$ , and  $\mathbf{v}$  are the diagonal mass matrix, viscous damping matrix, and relative displacement vector, respectively;  $m_i$  is the lumped mass associated with the  $i$ -th floor,  $\ddot{v}_{ii}$  is the total acceleration at the  $i$ -th floor. The kinetic energy and input energy are calculated as follows:

$$E_k = \frac{1}{2} \dot{\mathbf{v}}_t^T \mathbf{m} \dot{\mathbf{v}}_t = \frac{1}{2} \sum_{i=1}^N m_i (\dot{v}_{ii})^2 \quad (2.26a)$$

$$E_i = \int \left( \sum_{i=1}^N m_i \ddot{v}_{ii} \right) dv_g \quad (2.26b)$$

where  $E_k$  is the summation of the kinetic energy at each floor level, calculated using an absolute velocity ( $\dot{v}_{ii}$ ) at the  $i$ -th floor, and  $E_i$  is the summation of the work due to an inertia force ( $m_i \ddot{v}_{ii}$ ) at each floor for ground displacement.

Akiyama<sup>2</sup> has shown that the relative input energy  $E_i'$  based on a SDOF system can provide a very good estimate of the input energy for multi-story buildings. Although no parametric study is attempted here to verify the same conclusion for the absolute input energy  $E_i$ , shaking table test results for a six-story concentrically braced steel structure will be used to support this conclusion.

Figure 2.8 shows the 0.3-scale test model during the shaking table test; the 1978 Miyagi-Ken-Oki (MO) earthquake was used as the input ground motion. The test structure is classified by the UBC<sup>1</sup> as a dual system with two exterior ductile moment-resisting frames and one interior concentrically K-braced frame in the excitation direction. The magnitude of the earthquake record was scaled to different levels to represent different limit states of the structure responses. Details of the test results are reported in Reference 20. During the collapse level test (MO-65 Test, which had a measured peak base horizontal acceleration of 0.65g), the model experienced severe brace buckling in the bottom five stories, and the braces in the fifth story even ruptured. Figure 2.9 shows the envelope of base shear versus critical inter-story drift index obtained from different limit state tests. As a result of brace buckling and rupture, the envelope exhibits strength deterioration. Figure 2.10 shows the energy time histories of the MO-65 Test. Note that

the ‘‘viscous damped energy’’ curve was calculated indirectly by the following expression:

$$E_{\xi} = E_i - E_k - E_s - E_h . \quad (2.27)$$

In order to compare the experimental input energy of this frame with an elastic-perfectly plastic SDOF system, an estimate of the displacement ductility ratio for this frame from the test envelope in Fig. 2.9 is needed. If this nonlinear envelope is approximated by two linear segments, with the yield level calculated from simple plastic analysis,<sup>20</sup> the corresponding ductility ratio is 2.6. The calculated input energy spectrum of a SDOF system with a ductility ratio of 2.6 and a viscous damping ratio of 2%, which was the measured first mode equivalent viscous damping ratio, is shown in Fig. 2.11. The quantities presented in Fig. 2.11 have been scaled to the prototype level by similitude laws. The correlation between the experimentally measured  $V_i$  for the multi-story structure and the calculated  $V_i$  for a SDOF system is excellent. It is concluded from this case study that the input energy spectra for a SDOF system can be used to predict the input energy demand for this type of multi-story building structure reliably.



### III. ESTIMATION OF STRUCTURAL MEMBER ENERGY SUPPLY

#### 3.1. Introductory Remarks

In the energy-based seismic design methods proposed by previous researchers,<sup>2,10</sup> it is commonly assumed that the energy dissipation capacity (or supply) of each member can be predicted reliably; this capacity is assumed to be identical under cyclic loading to that provided under monotonic loading. Some test results are considered with the purpose of examining this assumption. Test results of a series of steel beams under the same type of deformation pattern but with varying amplitudes are examined first in order to study the effect of amplitude on the energy dissipation capacity of a structural member. To study the effect of deformation path on the energy dissipation capacity, test results for two identical shear walls and two identical composite beams are examined.

#### 3.2. Steel Beam Testing

A series of cantilever steel beams have been tested under strain reversal for different amplitudes.<sup>6</sup> The number of cycles required for the beam to fail versus strain amplitude is shown in Fig. 3.1. By ignoring strain hardening and Bauschinger effects a typical moment-curvature curve under cyclic loading can be idealized as shown in Fig. 3.2: these two factors tend to compensate each other from the standpoint of energy dissipation. The dissipated energy per unit length,  $e_d$ , is the area enclosed by the hysteresis loop:

$$e_d = \int M_p d\phi_p \approx 2M_p (2\phi_p) = 4M_p \phi_p \approx 4M_p \bar{\phi} \quad (3.1)$$

where  $M_p$  is the plastic moment,  $\phi_p$  is the plastic curvature, and  $\bar{\phi}$  is the controlling (constant) curvature, which from Fig. 3.1 is the sum of  $\phi_p$  and the yielding curvature  $\phi_y$ . Plastic curvature  $\phi_p$  is approximated by  $\bar{\phi}$  in Eq. 3.1; this is a reasonable assumption when the controlling curvature is much larger than the yielding curvature. By letting

$$\bar{\phi} = \frac{\bar{\epsilon}}{d/2} \quad (3.2)$$

where  $\bar{\epsilon}$  is the controlling strain at beam flange, and  $d$  is the beam depth, the total energy dissipated in  $n$  cycles ( $n$  = number of cycles required to rupture the beam), is

$$e_d = 4 M_p n \bar{\epsilon} \left( \frac{2}{d} \right) = \frac{8M_p}{d} (n \bar{\epsilon}) . \quad (3.3)$$

Figure 3.1 also shows the  $n\bar{\epsilon}$  versus  $\bar{\epsilon}$  curve. By assuming constant plastic hinge length  $L_p$  for all the specimens tested, the total energy dissipation capacity  $e_d L_p$  will be significantly smaller for beams subjected to larger amplitude cyclic deformations.

By extrapolating the energy dissipation capacity from the  $n\bar{\epsilon}$  curve for  $n = 1$ , which corresponds to the case of monotonic loading, it is concluded that the energy dissipation capacity is much lower than that provided under cyclic loading, especially when the ductility ratio is low. If energy were to be used as a criterion for design, the energy dissipation capacity of structural elements derived from monotonic loading tests would be too conservative.

### 3.3. Shear Wall Testing

Figure 3.3 shows the hysteretic behavior of two identical reinforced concrete shear wall structures tested under monotonic and cyclic loading.<sup>7</sup> Although Wall 3 has a larger ductility ratio, the total energy dissipation capacity of Wall 3 is only 60% of that of Wall 1. This demonstrates that the energy dissipation capacity of a structural element is highly dependent on the loading path, the deformation path or both.

### 3.4. Composite Beam Testing

Figure 3.4 shows the load-deformation curves of two 0.3-scale composite beams tested under different deformation paths.<sup>20</sup> The first beam (CG1) experienced large displacement ductility in the first half cycle, followed by reversed loading in the opposite direction that caused severe flange local buckling. The energy dissipated is 27 kip-in. The second beam (CG3) was subjected to two complete cycles of loading reversals with displacement ductility smaller than that imposed on CG1. Another five complete cycles with displacement ductility similar to that imposed on CG1 were then applied. The energy dissipated in this beam is 128 kip-in, 4.7 times larger than that dissipated by CG1.

Strictly speaking, the comparison made above for these two composite beams is questionable. There is no reason why CG1 cannot dissipate more energy although it suffers flange local buckling when loaded into the reverse direction. Although the test of CG1 was terminated when strength deterioration was observed, it is believed that if a similar deformation path to that of CG3 but with higher displacement amplitudes were applied to CG1, the energy dissipation capacity would be smaller.

### **3.5. Concluding Remarks**

These experimental results demonstrate that energy dissipation capacity is not constant and depends on loading path or deformation path or both. From analysis of available test results it appears that for properly designed and detailed structures, the energy dissipation capacity under monotonic loading is a lower limit on the energy dissipation capacity under cyclic loading or inelastic deformation or both. However the use of this lower limit could be too conservative for earthquake-resistant design, particularly if the ductility ratio is limited to low values with respect to the ductility ratio reached under monotonic loading. Thus, efforts should be devoted to determining experimentally the energy dissipation capacity of main structural elements as a function of the maximum deformation ductility that can be tolerated, and the relationship between energy dissipation capacity and loading and deformation paths.

## IV. CONCLUSIONS

From the results obtained in the studies that have been summarized in this report, the following observations can be made.

- (1) The use of an "absolute" energy equation rather than a "relative" energy equation has the advantage that the physical energy input is reflected.
- (2) The profiles of the energy time histories calculated by the absolute energy equation differ significantly from those calculated by the conventional relative energy equation (see Fig. 2.2.)
- (3) The absolute and the relative input energies for a constant displacement ductility are very close in the period range of practical interest, namely 0.3 to 5.0 sec (from Fig. 2.3.) The difference between these two input energies increases as the structure period differs more and more from the previous range. As the period decreases, the absolute input energy approaches  $m\dot{v}_{g(max)}^2/2$ , where  $\dot{v}_{g(max)}$  is the maximum ground velocity, and the relative input energy approaches zero. The situation is reversed for long period structures.
- (4) For certain types of earthquake ground motion, the absolute input energy spectra are sensitive to the variation of ductility ratio.
- (5) Except for the highly harmonic earthquakes (1985 Mexico City earthquake for example), the absolute input energy spectra for a constant ductility ratio can be predicted reliably by the elastic input energy spectra using Iwan's procedure which takes into consideration the effect of increasing damping ratio and natural period.
- (6) The maximum energy input to a structure whose fundamental period is close to the predominant excitation period of an expected earthquake can be predicted reliably with the expected maximum ground velocity and the amplification factor  $\Psi$  (one such expression for ductility ratio 5 and damping ratio 5 percent is presented in Eq. 2.24.) The amplification factor  $\Psi$  is approximately linearly related to the strong motion duration  $t_D$  defined in Eq. 2.22.

- (7) For medium rise steel dual systems it is possible to estimate with sufficient accuracy the input energy to a multi-story building from the SDOF absolute input energy spectra using the fundamental period of the multi-story structure.
- (8) The energy dissipation capacity of a structural member is not unique and depends on the loading or deformation paths or both. The energy dissipation capacity of a member under monotonic loading can only provide a lower bound estimate and may significantly underestimate its energy dissipation capacity, especially when the ductility ratio is limited to values that are low compared with the ductility ratio reached under monotonic loading.
- (9) There is an urgent need to determine the energy dissipation capacity of the main types of structural elements and structural systems as a function of the maximum deformation ductility that can be tolerated and of the dynamic characteristics of the actual ground motions.

## REFERENCES

1. *Uniform Building Code*, International Conference of Building Officials, Whittier, California, 1985.
2. Akiyama, H., *Earthquake Resistant Limit-State Design for Buildings*, University of Tokyo Press, 1985.
3. Anderson, J. C. and Bertero, V. V., "Seismic Behavior of Multistory Frames by Different Philosophies," *Report No. UCB/EERC-69/11*, Earthquake Engineering Research Center, University of California, Berkeley, California, October, 1969.
4. Arias, A., "A Measure of Earthquake Intensity," in *Seismic Design for Nuclear Power Plants*, ed. R.J. Hansen, pp. 438-469, Massachusetts Institute of Technology Press, Cambridge, Mass., 1970.
5. Berg, G. V. and Thomaidis, S. S., "Energy Consumption by Structures in Strong-Motion Earthquakes," *Proceedings of the Second World Conference on Earthquake Engineering*, pp. 681-696, Tokyo, Japan, 1960.
6. Bertero, V. V. and Popov, E. P., "Effect of Large Alternating Strains on Steel Beams," *Proceedings*, vol. 91, no. ST1, pp. 1-12, ASCE, February, 1965.
7. Bertero, V. V., Popov, E. P., Wang, T. Y., and Vallenias, J. M., "Seismic Design Implications of Hysteretic Behavior of Reinforced Concrete Structural Walls," *Proceedings of the Sixth World Conference on Earthquake Engineering*, pp. 10-19, New Delhi, India, January, 1977.
8. Goel, S. C. and Berg, G. V., "Inelastic Earthquake Response of Tall Steel Frames," *Journal of the Structural Division*, vol. 94, no. ST8, pp. 1907-1834, ASCE, August, 1968.
9. Hadjian, A. H., "A Re-evaluation of Equivalent Linear Models for Simple Yielding Systems," *Earthquake Engineering and Structural Dynamics*, vol. 10, pp. 759-767, 1982.
10. Housner, G. W., "Limit Design of Structures to Resist Earthquake," *Proceedings of the First World Conference on Earthquake Engineering*, pp. 5-1 to 5-13, Berkeley, California,

1956.

11. Iwan, W. D., "Estimating Inelastic Response Spectra from Elastic Spectra," *Earthquake Engineering and Structural Dynamics*, vol. 8, pp. 375-388, 1980.
12. Jennings, P. C., "Earthquake Response of a Yielding Structure," *Journal of the Engineering Mechanics Division*, vol. 90, no. EM4, pp. 41-68, ASCE, August, 1965.
13. Kato, B. and Akiyama, H., "Seismic Design of Steel Buildings," *Journal of the Structural Division*, vol. 108, no. ST8, pp. 1709-1721, ASCE, August, 1982.
14. Mahin, S. A. and Lin, J., "Construction of Inelastic Response Spectrum for Single Degree of Freedom System," *Report No. UCB/EERC-83/17*, Earthquake Engineering Research Center, University of California, Berkeley, March, 1983.
15. McKeivitt, W. E., Anderson, D. L., Nathan, N. D., and Cherry, S., "Towards a Simple Energy Method for Seismic Design of Structures," *Proceedings of the Second U. S. National Conference on Earthquake Engineering*, pp. 383-392, EERI, 1979.
16. Newmark, N. M. and Hall, W. J., "Procedures and Criteria for Earthquake Resistant Design," *Building Science Series No. 46*, pp. 209-236, Building Practices for Disaster Mitigation, National Bureau of Standards, February, 1973.
17. Pecknold, D. A. and Riddle, R., "Effect of Initial Base Motion on Response Spectra," *Journal of the Engineering Mechanics Division*, vol. 104, no. EM2, pp. 485-491, ASCE, April, 1978.
18. Tembulkar, J. M. and Nau, J. M., "Inelastic Modeling and Seismic Energy Dissipation," *Journal of the Structural Engineering*, vol. 113, no. 6, pp. 1373-1377, ASCE, June, 1987.
19. Trifunac, M. D. and Brady, A. G., "A Study on the Duration of Strong Earthquake Ground Motion," *Bulletin of the Seismological Society of America*, vol. 65, no. 3, pp. 581-626, June, 1975.
20. Uang, C.-M and Bertero, V. V., "Earthquake Simulation Tests and Associated Studies of a 0.3-Scale Model of a 6-Story Concentrically Braced Steel Structure," *Report No. UCB/EERC-86/10*, Earthquake Engineering Research Center, University of California, Berkeley, California, December 1986.

21. Veletsos, A. S., Newmark, N. M., and Chelapati, C. V., "Deformation Spectra for Elastic and Elastoplastic Systems Subjected to Ground Shock and Earthquake Motions," *Proceedings of the Third World Conference on Earthquake Engineering*, pp. II-663 to II-678, Wellington, New Zealand, 1965.
22. Zahrah, T. F. and Hall, W. J., "Seismic Energy Absorption in Simple Structures," *Structural Research Series No. 501*, University of Illinois, Urbana, Illinois, July, 1982.



## APPENDIX - NOTATION

$c$	viscous damping coefficient
$\mathbf{c}$	viscous damping matrix
$d$	beam depth
$e_d$	hysteretic dissipated energy of a steel beam
$E_a$	absorbed energy, ( $= E_s + E_h$ )
$E_D$	maximum elastic energy stored in a SDOF system
$E_h$	hysteretic dissipated energy
$E_i$	absolute input energy
$E'_i$	relative input energy
$E_k$	absolute kinetic energy
$E'_k$	relative kinetic energy
$E_s$	recoverable elastic strain energy
$E_\xi$	damping energy
$f_s$	restoring force
$\mathbf{f}_s$	restoring force vector
$I_A$	Arias intensity
$m$	lumped floor mass
$\mathbf{m}$	mass matrix of an $N$ -story building structure
$M_p$	plastic moment
$S_{pv}$	linear elastic pseudo-velocity
$S_d$	linear elastic spectral displacement
$t_d$	total duration of an earthquake record
$t_D$	strong motion duration of an earthquake record
$T_e$	equivalent period
$T$	small-amplitude (or elastic) period
$v$	relative structural displacement
$\mathbf{v}$	relative structural displacement vector

$\dot{v}$	relative structural velocity
$\ddot{v}$	relative structural acceleration
$v_t$	absolute structural displacement
$\dot{v}_t$	absolute structural velocity
$\ddot{v}_t$	absolute structural acceleration
$v_g$	earthquake ground displacement
$\dot{v}_g$	earthquake ground velocity
$\dot{v}_{g(max)}$	maximum earthquake ground velocity
$\ddot{v}_g$	earthquake ground acceleration
$V_i$	absolute input energy equivalent velocity, ( $= \sqrt{(2E_i)/m}$ )
$V'_i$	relative input energy equivalent velocity, ( $= \sqrt{(2E'_i)/m}$ )
$\xi$	nominal viscous damping ratio
$\xi_e$	equivalent viscous damping
$\phi$	curvature
$\phi_p$	plastic curvature
$\phi_y$	yield curvature
$\bar{\epsilon}$	controlling flange strain
$\Psi$	amplification factor of $V_i$ above $\dot{v}_{g(max)}$

No.	Earthquake	Record	Comp.	Focal Depth (km)	$M_s$	MMI	Geology	Epicentral Distance (km)	$t_p$ (sec)
1	Imperial Valley May 18, 1940	El Centro	N00E	16.0	6.3	VII-VIII	30m stiff clay volcanic rock	9.3	244
2	Mexico City September 19, 1985	SCT	N90E	4.2-5.0	8.1	IX	Soft lacustrine clay	360	38.8
3	San Salvador October 10, 1986	CIG	N90E	8.0	5.4	VIII-IX	Fluvialite pumice	9.0	4.3
4	San Fernando February 9, 1971	Pacoima Dam	S16E	13.0 to surface	6.6	IX-X	Highly jointed diorite gneiss	9.1	6.7
5	Kern County July 21, 1952	Taft	N21E	16.0	7.7	VII	Alluvium	43	30.5

Table 1.1 Earthquake Record Data

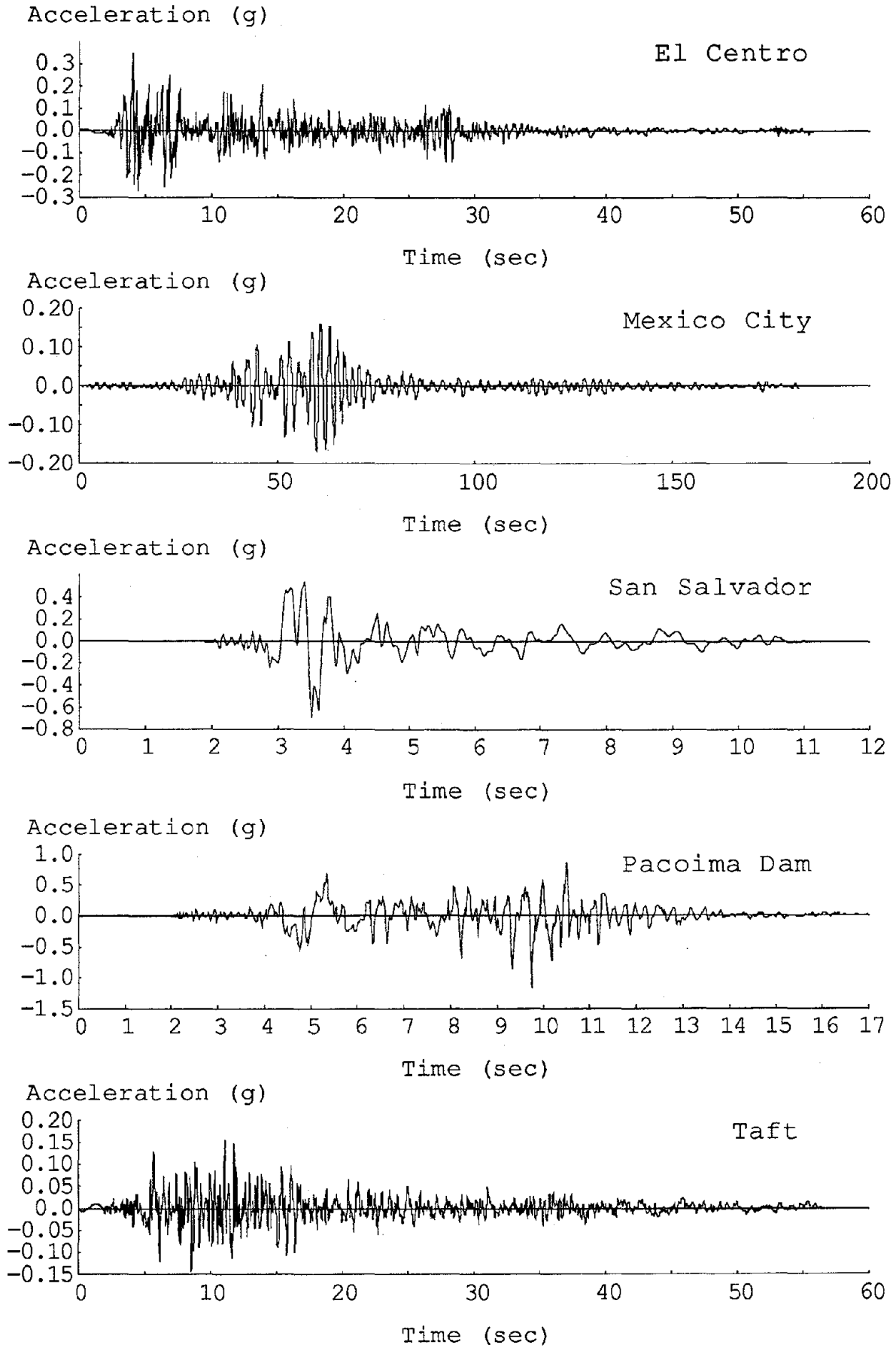


Fig. 1.1 Earthquake Ground Motion Acceleration Time Histories

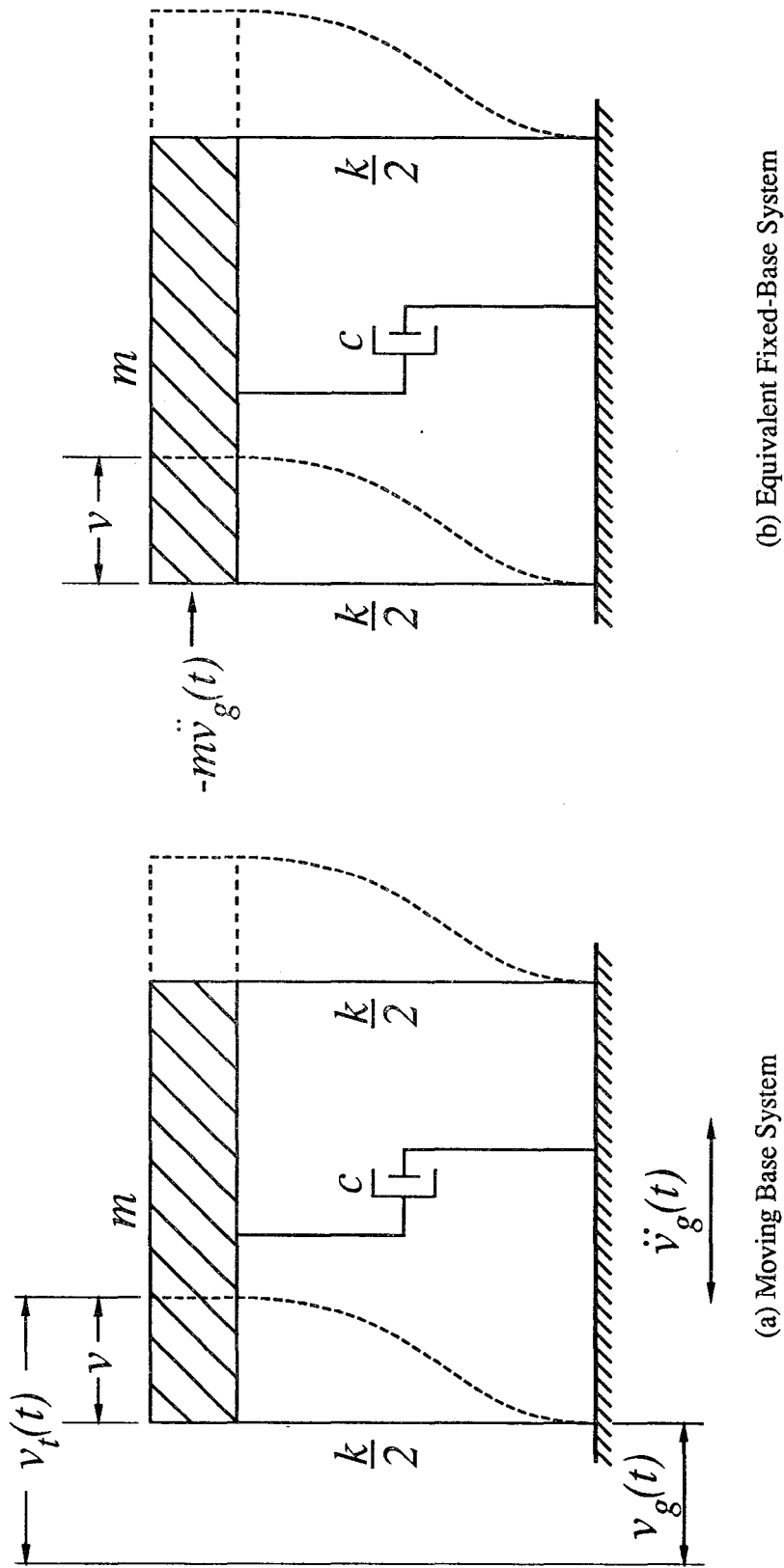
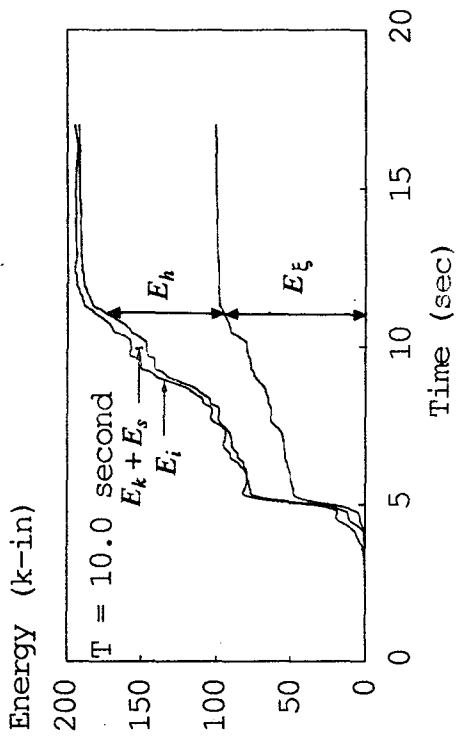
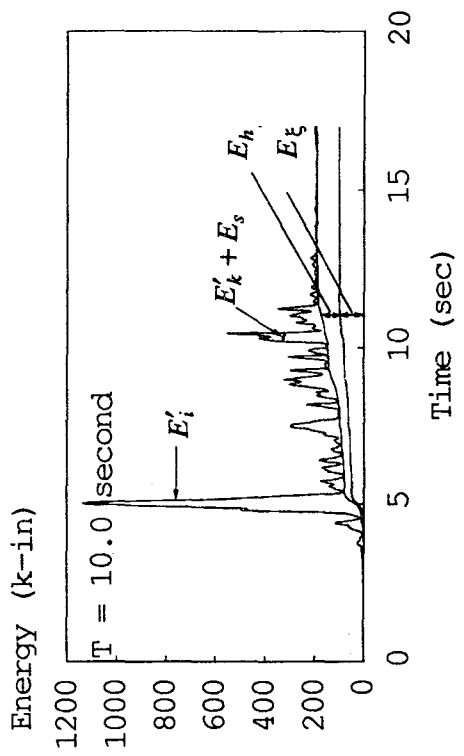


Fig. 2.1 Mathematical Model of a SDOF System Subjected to an Earthquake Ground Motion



(a) Energy Terms Defined by Method 1



(b) Energy Terms Defined by Method 2

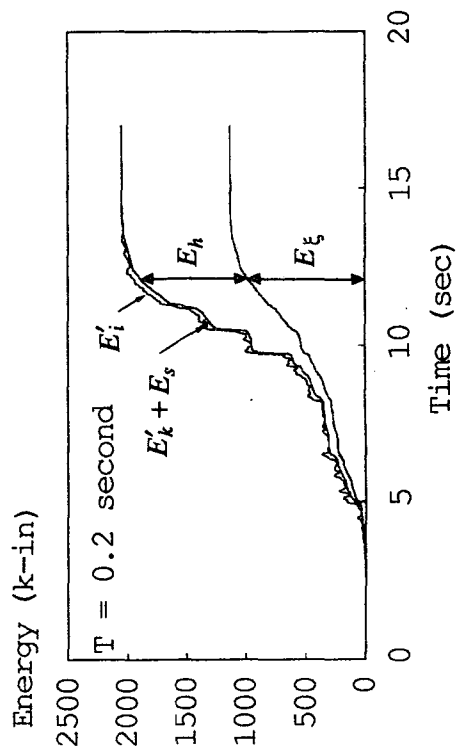
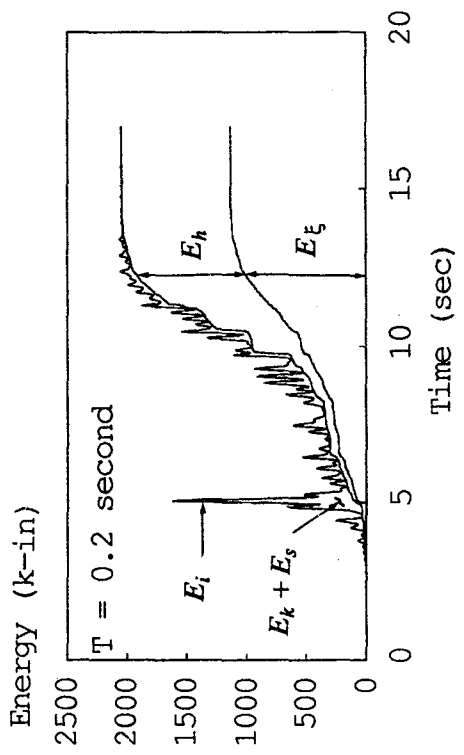


Fig. 2.2 Energy Time Histories for an Elastic-Perfectly Plastic System subjected to the 1971

San Fernando Earthquake — Pacoima Dam Record (Ductility Ratio 3, 5% Damping)

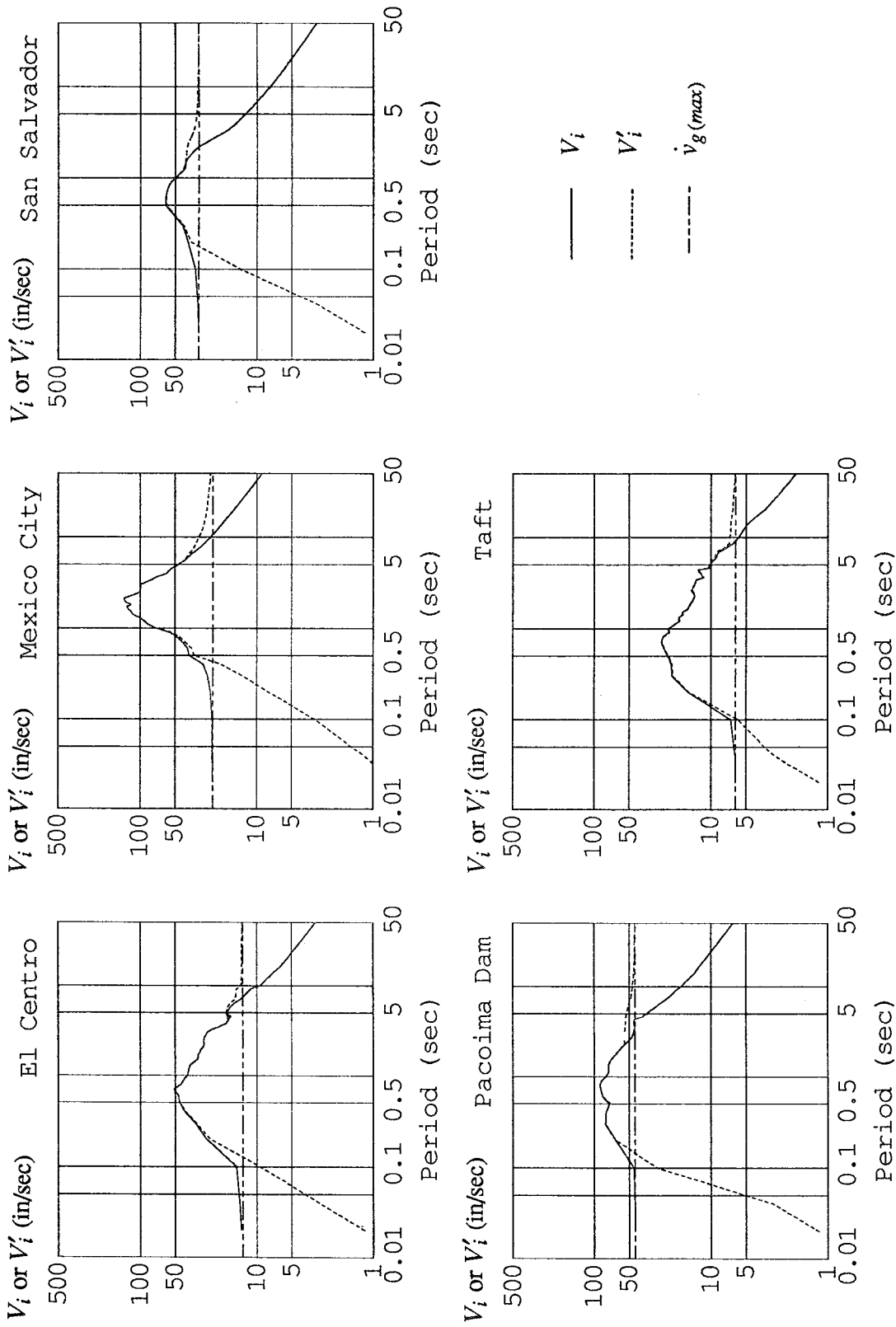


Fig. 2.3 Comparison of Input Energy Equivalent Velocity Spectra for Ductility Ratio 5 (5% Damping)

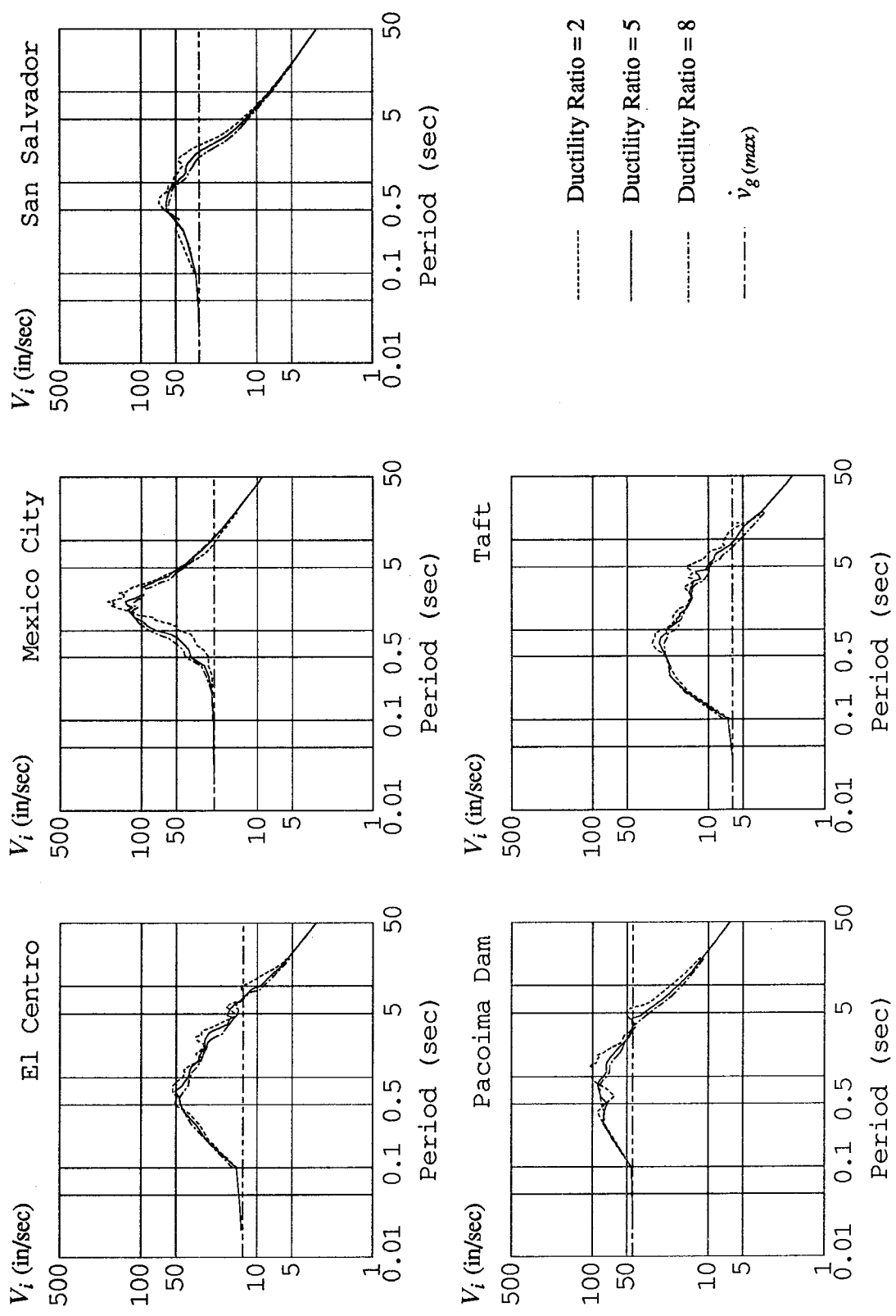


Fig. 2.4 Comparison of Absolute Input Energy Equivalent Velocity Spectra for Ductility Ratios 2, 5, and 8 (5% Damping)



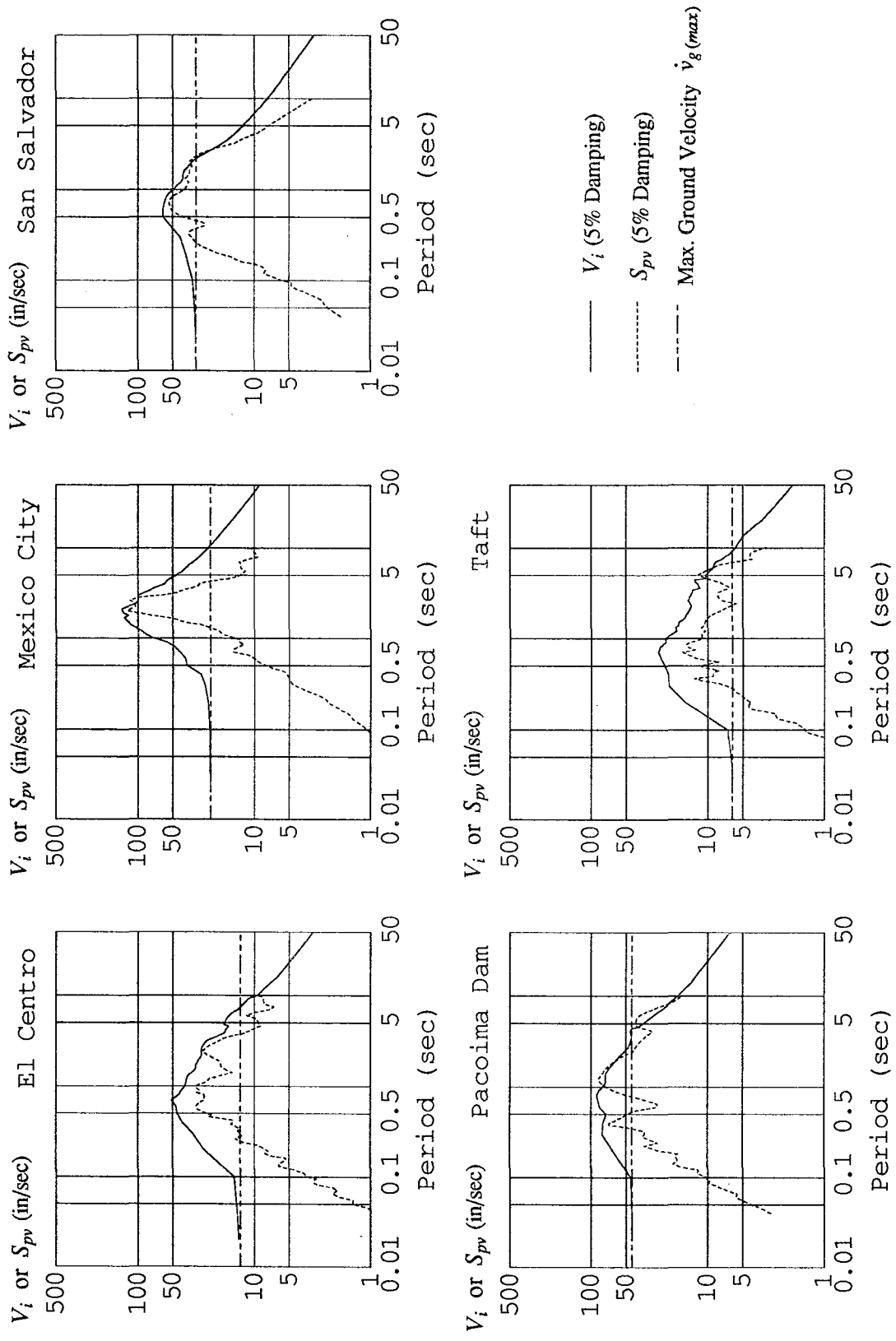


Fig. 2.5 Comparison of Absolute Input Energy Equivalent Velocity Spectra and Linear Elastic Pseudo-velocity Response Spectra for Ductility Ratio 5 (5% Damping)

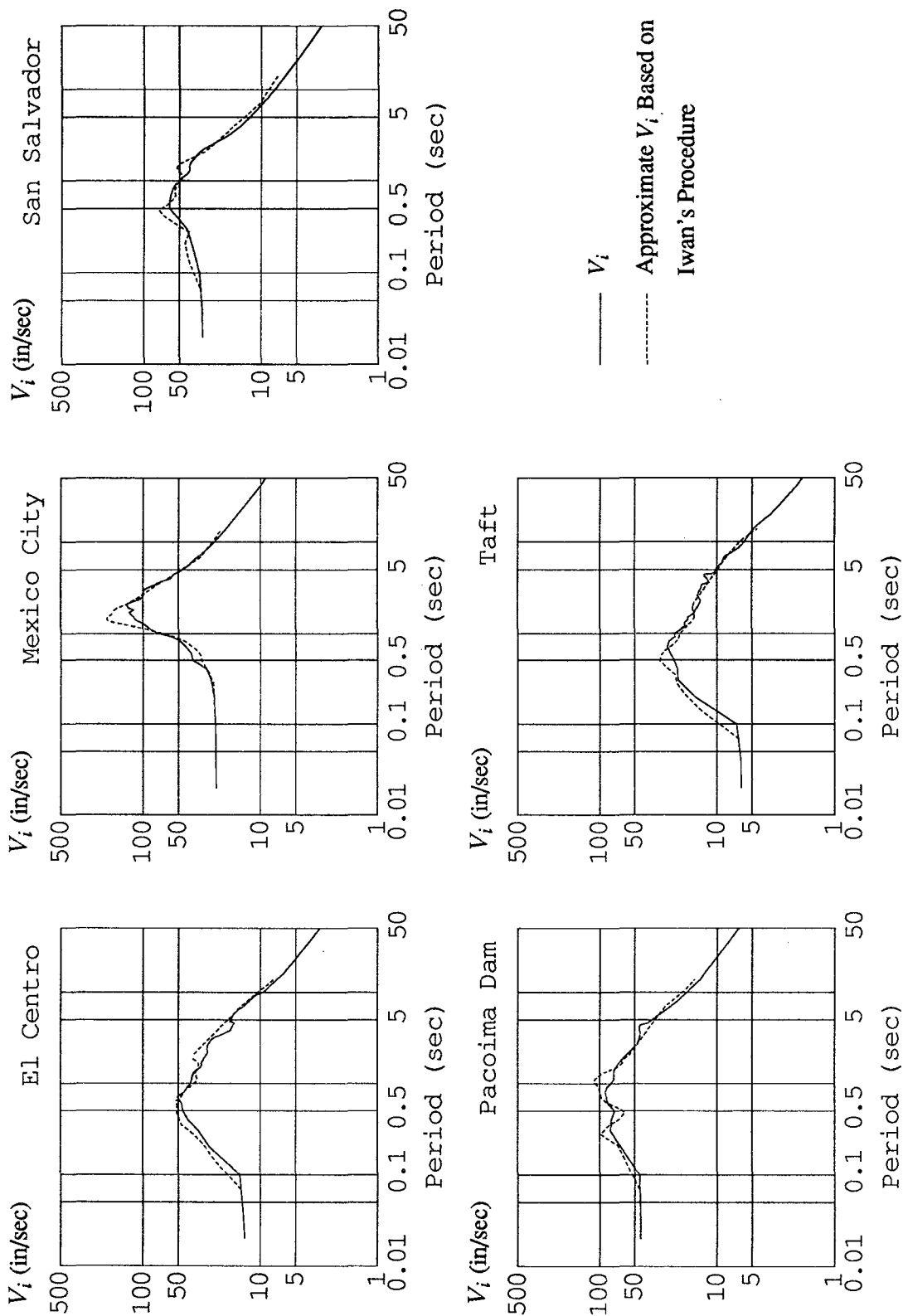


Fig. 2.6 Comparison of Absolute Input Energy and Iwan's Elastic Input Energy Equivalent Velocity Response Spectra for Ductility Ratio 5 (5% Damping)

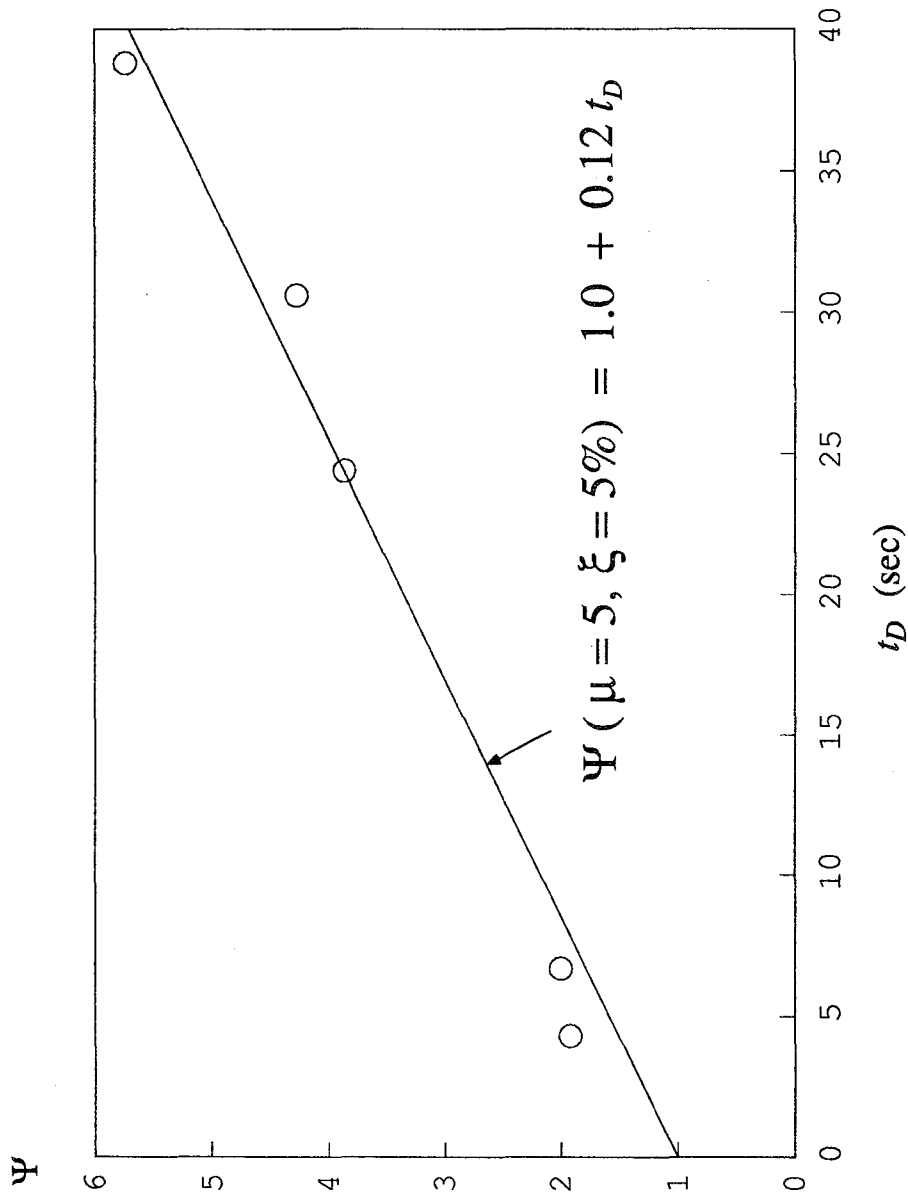


Fig. 2.7 Input Energy Equivalent Velocity Amplification Factor and Strong Motion Duration Relationship

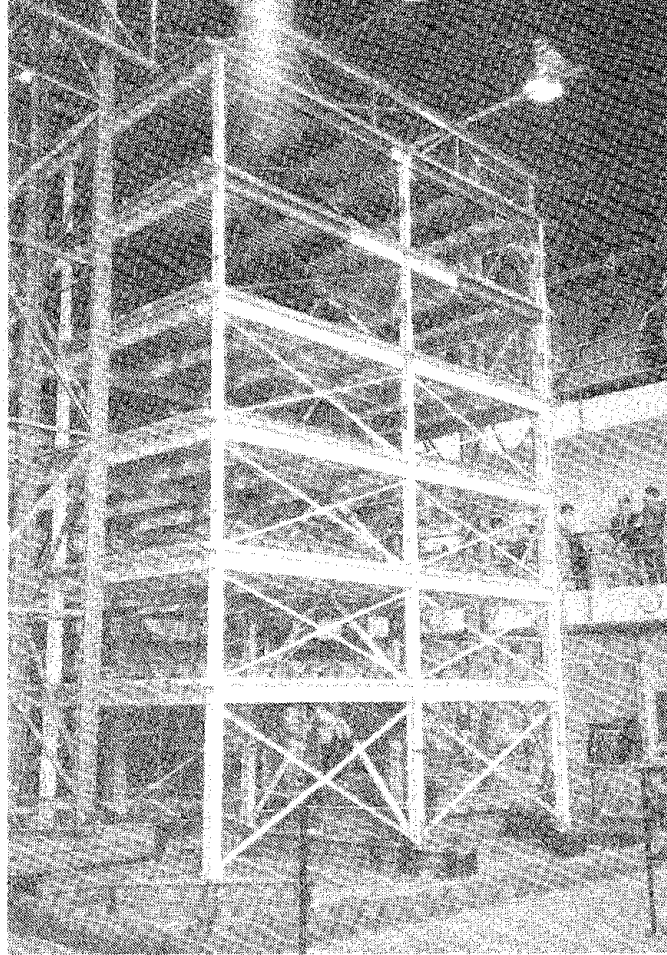


Fig. 2.8 Overall View of 0.3-Scale Model with Reference Frame<sup>20</sup>

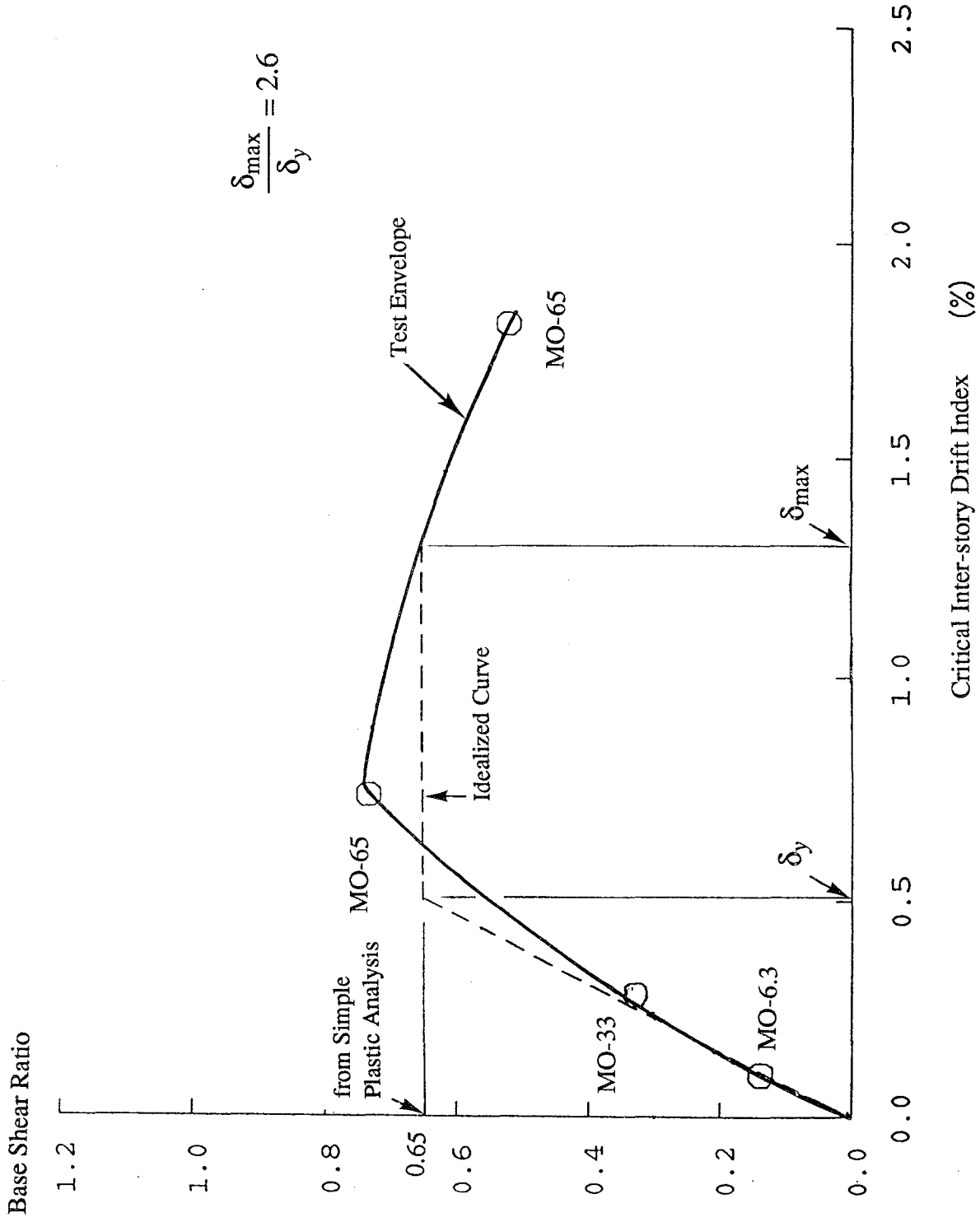


Fig. 2.9 Envelope of Critical Inter-story Drift Index versus Base Shear Ratio<sup>20</sup>

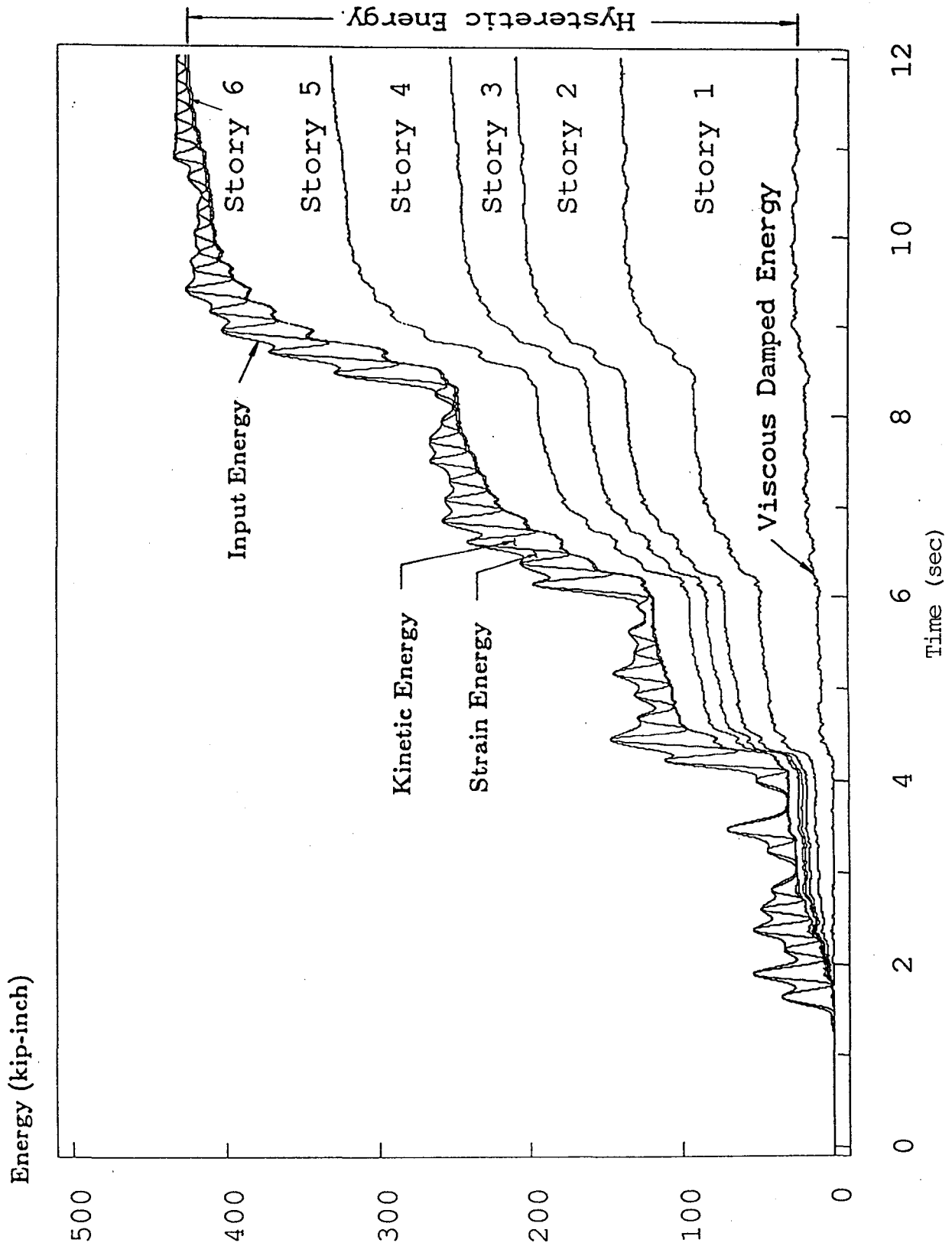


Fig. 2.10 Model Collapse Level Test (MO-65 Test) Energy Time Histories<sup>20</sup>

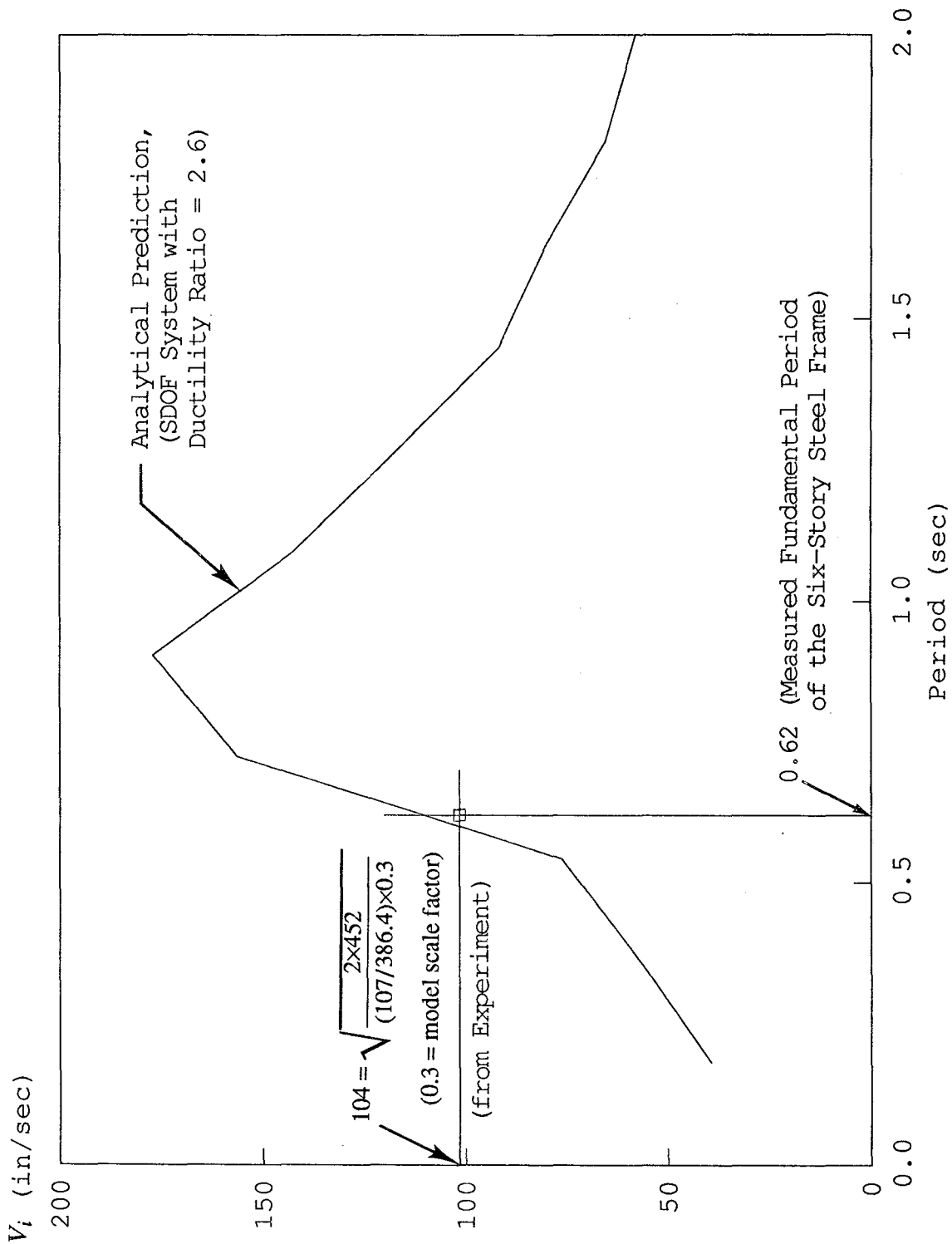


Fig. 2.11 Comparison of Analytical and Experimental Input Energy Equivalent Velocities  
 (Measured Ground Motion during MO-65 Test, 2% Damping Ratio)

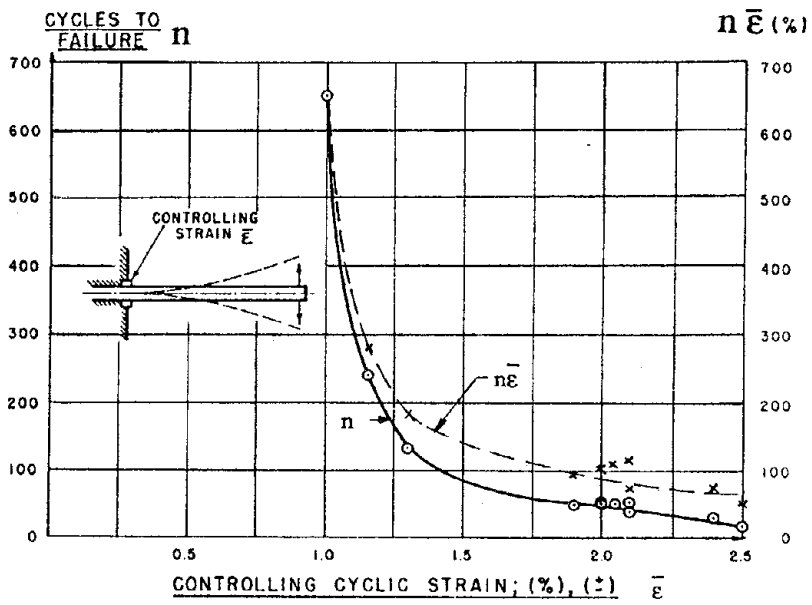


Fig. 3.1 Number of Cycles Required to Attain Fracture as a Function of the Controlling Strain<sup>6</sup>

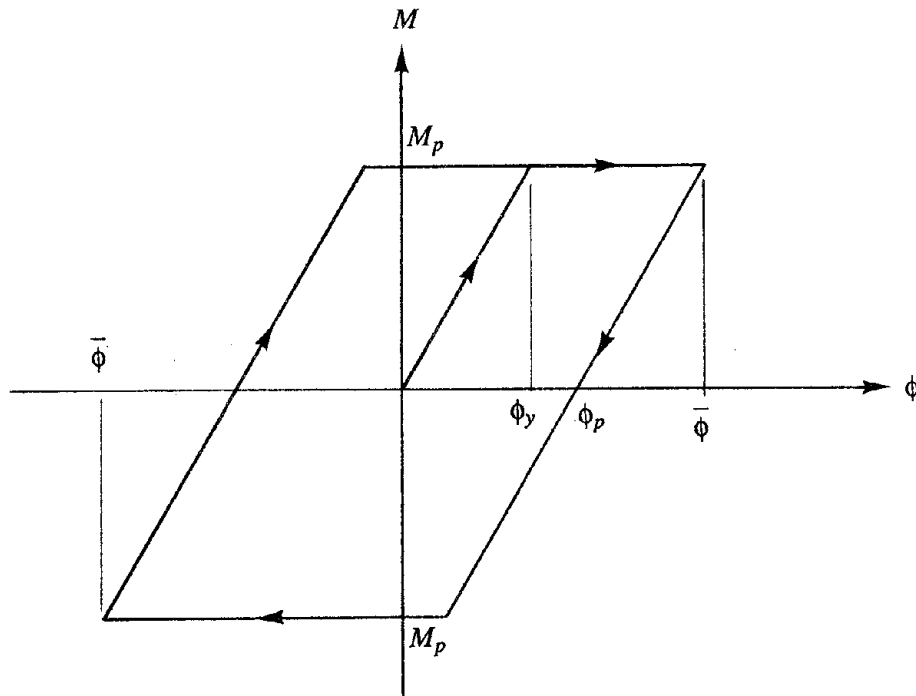


Fig. 3.2 Idealized Steel Beam Moment-Curvature Relationship



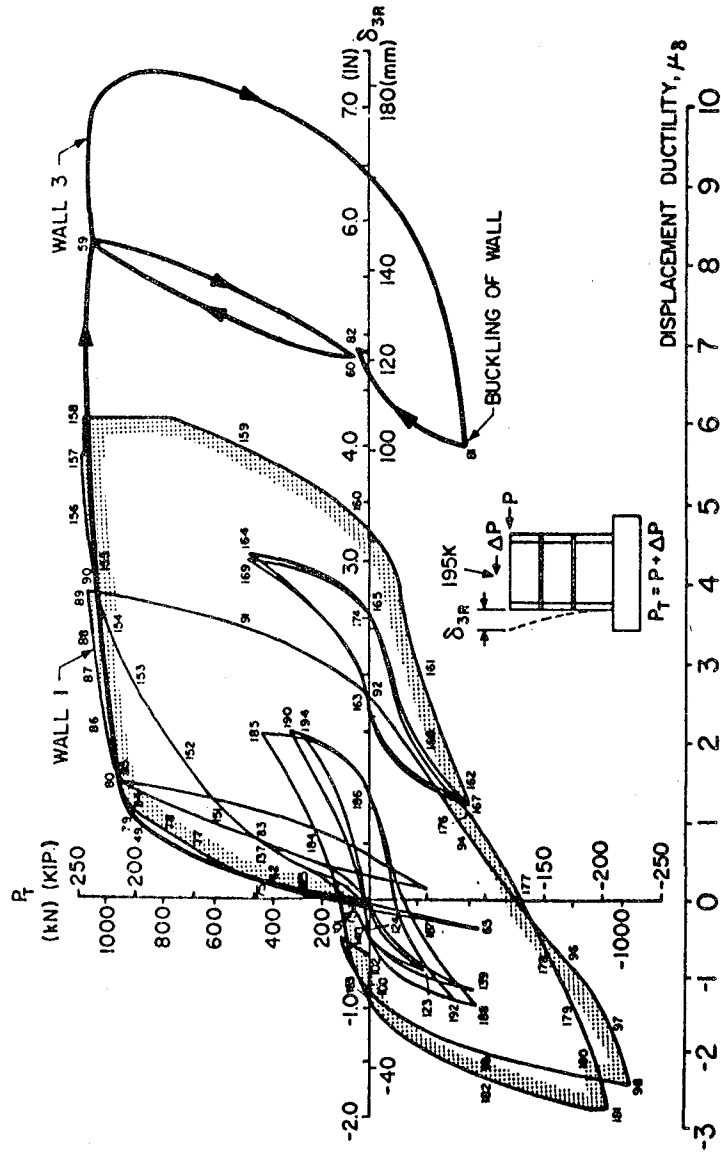
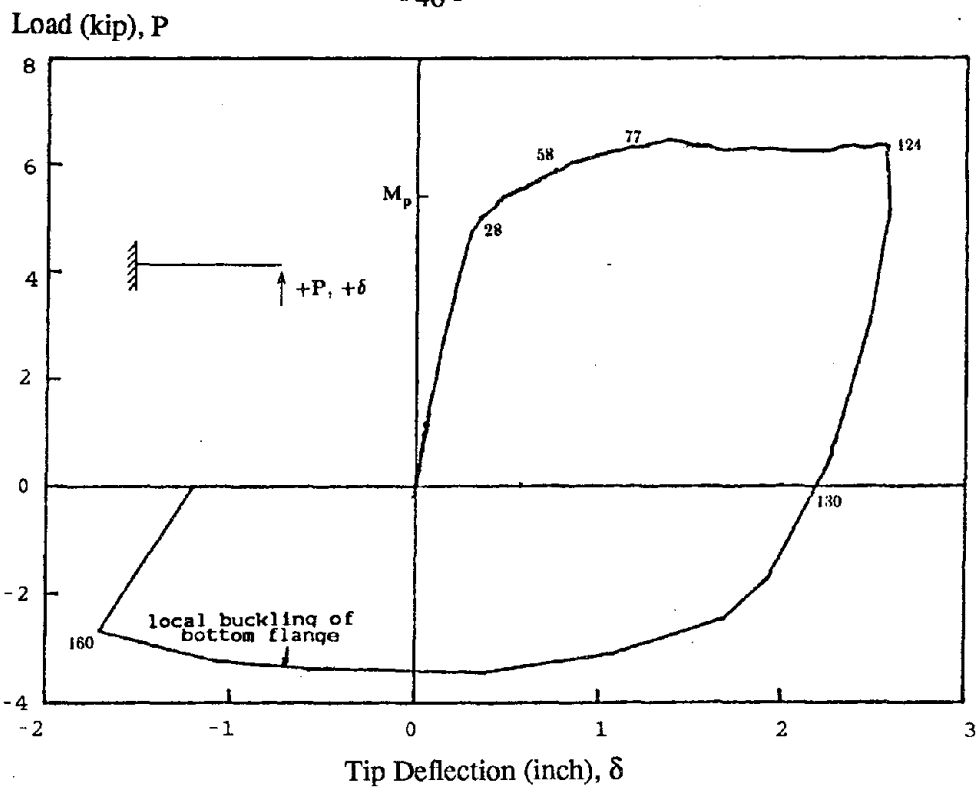
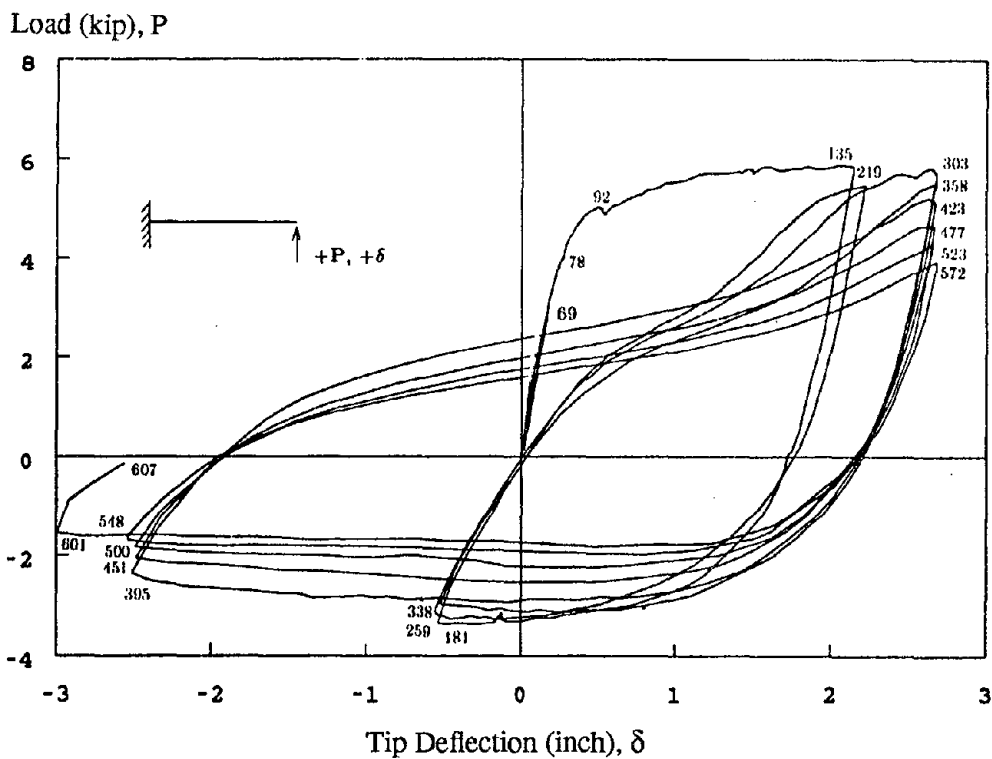


Fig. 3.3 Comparison of Energy Dissipation Capacities of Two Shear Walls<sup>7</sup>

(Wall 1: Cyclic Loading; Wall 3: Monotonic Loading)



(a) Load versus Deflection Curve of CG1



(b) Load versus Deflection Curve of CG3

Fig. 3.4 Comparison of Energy Dissipation Capacities of Two Composite Girders<sup>20</sup>

## EARTHQUAKE ENGINEERING RESEARCH CENTER REPORT SERIES

EERC reports are available from the National Information Service for Earthquake Engineering (NISEE) and from the National Technical Information Service (NTIS). Numbers in parentheses are Accession Numbers assigned by the National Technical Information Service; these are followed by a price code. Contact NTIS, 5285 Port Royal Road, Springfield Virginia, 22161 for more information. Reports without Accession Numbers were not available from NTIS at the time of printing. For a current complete list of EERC reports (from EERC 67-1) and availability information, please contact University of California, EERC, NISEE, 1301 South 46th Street, Richmond, California 94804.

- UCB/EERC-80/01 "Earthquake Response of Concrete Gravity Dams Including Hydrodynamic and Foundation Interaction Effects," by Chopra, A.K., Chakrabarti, P. and Gupta, S., January 1980, (AD-A087297)A10.
- UCB/EERC-80/02 "Rocking Response of Rigid Blocks to Earthquakes," by Yim, C.S., Chopra, A.K. and Penzien, J., January 1980, (PB80 166 002)A04.
- UCB/EERC-80/03 "Optimum Inelastic Design of Seismic-Resistant Reinforced Concrete Frame Structures," by Zagajski, S.W. and Bertero, V.V., January 1980, (PB80 164 635)A06.
- UCB/EERC-80/04 "Effects of Amount and Arrangement of Wall-Panel Reinforcement on Hysteretic Behavior of Reinforced Concrete Walls," by Iliya, R. and Bertero, V.V., February 1980, (PB81 122 525)A09.
- UCB/EERC-80/05 "Shaking Table Research on Concrete Dam Models," by Niwa, A. and Clough, R.W., September 1980, (PB81 122 368)A06.
- UCB/EERC-80/06 "The Design of Steel Energy-Absorbing Restrainers and their Incorporation into Nuclear Power Plants for Enhanced Safety (Vol 1a): Piping with Energy Absorbing Restrainers: Parameter Study on Small Systems," by Powell, G.H., Oughourlian, C. and Simons, J., June 1980.
- UCB/EERC-80/07 "Inelastic Torsional Response of Structures Subjected to Earthquake Ground Motions," by Yamazaki, Y., April 1980, (PB81 122 327)A08.
- UCB/EERC-80/08 "Study of X-Braced Steel Frame Structures under Earthquake Simulation," by Ghanaat, Y., April 1980, (PB81 122 335)A11.
- UCB/EERC-80/09 "Hybrid Modelling of Soil-Structure Interaction," by Gupta, S., Lin, T.W. and Penzien, J., May 1980, (PB81 122 319)A07.
- UCB/EERC-80/10 "General Applicability of a Nonlinear Model of a One Story Steel Frame," by Sveinsson, B.I. and McNiven, H.D., May 1980, (PB81 124 877)A06.
- UCB/EERC-80/11 "A Green-Function Method for Wave Interaction with a Submerged Body," by Kioka, W., April 1980, (PB81 122 269)A07.
- UCB/EERC-80/12 "Hydrodynamic Pressure and Added Mass for Axisymmetric Bodies," by Nilrat, F., May 1980, (PB81 122 343)A08.
- UCB/EERC-80/13 "Treatment of Non-Linear Drag Forces Acting on Offshore Platforms," by Dao, B.V. and Penzien, J., May 1980, (PB81 153 413)A07.
- UCB/EERC-80/14 "2D Plane/Axisymmetric Solid Element (Type 3-Elastic or Elastic-Perfectly Plastic) for the ANSR-II Program," by Mondkar, D.P. and Powell, G.H., July 1980, (PB81 122 350)A03.
- UCB/EERC-80/15 "A Response Spectrum Method for Random Vibrations," by Der Kiureghian, A., June 1981, (PB81 122 301)A03.
- UCB/EERC-80/16 "Cyclic Inelastic Buckling of Tubular Steel Braces," by Zayas, V.A., Popov, E.P. and Mahin, S.A., June 1981, (PB81 124 885)A10.
- UCB/EERC-80/17 "Dynamic Response of Simple Arch Dams Including Hydrodynamic Interaction," by Porter, C.S. and Chopra, A.K., July 1981, (PB81 124 000)A13.
- UCB/EERC-80/18 "Experimental Testing of a Friction Damped Asismic Base Isolation System with Fail-Safe Characteristics," by Kelly, J.M., Beucke, K.E. and Skinner, M.S., July 1980, (PB81 148 595)A04.
- UCB/EERC-80/19 "The Design of Steel Energy-Absorbing Restrainers and their Incorporation into Nuclear Power Plants for Enhanced Safety (Vol.1B): Stochastic Seismic Analyses of Nuclear Power Plant Structures and Piping Systems Subjected to Multiple Supported Excitations," by Lee, M.C. and Penzien, J., June 1980, (PB82 201 872)A08.
- UCB/EERC-80/20 "The Design of Steel Energy-Absorbing Restrainers and their Incorporation into Nuclear Power Plants for Enhanced Safety (Vol 1C): Numerical Method for Dynamic Substructure Analysis," by Dickens, J.M. and Wilson, E.L., June 1980.
- UCB/EERC-80/21 "The Design of Steel Energy-Absorbing Restrainers and their Incorporation into Nuclear Power Plants for Enhanced Safety (Vol 2): Development and Testing of Restraints for Nuclear Piping Systems," by Kelly, J.M. and Skinner, M.S., June 1980.
- UCB/EERC-80/22 "3D Solid Element (Type 4-Elastic or Elastic-Perfectly-Plastic) for the ANSR-II Program," by Mondkar, D.P. and Powell, G.H., July 1980, (PB81 123 242)A03.
- UCB/EERC-80/23 "Gap-Friction Element (Type 5) for the Ansr-II Program," by Mondkar, D.P. and Powell, G.H., July 1980, (PB81 122 285)A03.
- UCB/EERC-80/24 "U-Bar Restraint Element (Type 11) for the ANSR-II Program," by Oughourlian, C. and Powell, G.H., July 1980, (PB81 122 293)A03.
- UCB/EERC-80/25 "Testing of a Natural Rubber Base Isolation System by an Explosively Simulated Earthquake," by Kelly, J.M., August 1980, (PB81 201 360)A04.
- UCB/EERC-80/26 "Input Identification from Structural Vibrational Response," by Hu, Y., August 1980, (PB81 152 308)A05.
- UCB/EERC-80/27 "Cyclic Inelastic Behavior of Steel Offshore Structures," by Zayas, V.A., Mahin, S.A. and Popov, E.P., August 1980, (PB81 196 180)A15.
- UCB/EERC-80/28 "Shaking Table Testing of a Reinforced Concrete Frame with Biaxial Response," by Oliva, M.G., October 1980, (PB81 154 304)A10.
- UCB/EERC-80/29 "Dynamic Properties of a Twelve-Story Prefabricated Panel Building," by Bouwkamp, J.G., Kollegger, J.P. and Stephen, R.M., October 1980, (PB82 138 777)A07.
- UCB/EERC-80/30 "Dynamic Properties of an Eight-Story Prefabricated Panel Building," by Bouwkamp, J.G., Kollegger, J.P. and Stephen, R.M., October 1980, (PB81 200 313)A05.
- UCB/EERC-80/31 "Predictive Dynamic Response of Panel Type Structures under Earthquakes," by Kollegger, J.P. and Bouwkamp, J.G., October 1980, (PB81 152 316)A04.
- UCB/EERC-80/32 "The Design of Steel Energy-Absorbing Restrainers and their Incorporation into Nuclear Power Plants for Enhanced Safety (Vol 3): Testing of Commercial Steels in Low-Cycle Torsional Fatigue," by Spanner, P., Parker, E.R., Jongewaard, E. and Dory, M., 1980.

- UCB/EERC-80/33 "The Design of Steel Energy-Absorbing Restrainers and their Incorporation into Nuclear Power Plants for Enhanced Safety (Vol 4): Shaking Table Tests of Piping Systems with Energy-Absorbing Restrainers," by Stierner, S.F. and Godden, W.G., September 1980, (PB82 201 880)A05.
- UCB/EERC-80/34 "The Design of Steel Energy-Absorbing Restrainers and their Incorporation into Nuclear Power Plants for Enhanced Safety (Vol 5): Summary Report," by Spencer, P., 1980.
- UCB/EERC-80/35 "Experimental Testing of an Energy-Absorbing Base Isolation System," by Kelly, J.M., Skinner, M.S. and Beucke, K.E., October 1980, (PB81 154 072)A04.
- UCB/EERC-80/36 "Simulating and Analyzing Artificial Non-Stationary Earth Ground Motions," by Nau, R.F., Oliver, R.M. and Pister, K.S., October 1980, (PB81 153 397)A04.
- UCB/EERC-80/37 "Earthquake Engineering at Berkeley - 1980," by , September 1980, (PB81 205 674)A09.
- UCB/EERC-80/38 "Inelastic Seismic Analysis of Large Panel Buildings," by Schricker, V. and Powell, G.H., September 1980, (PB81 154 338)A13.
- UCB/EERC-80/39 "Dynamic Response of Embankment, Concrete-Gavity and Arch Dams Including Hydrodynamic Interaction," by Hall, J.F. and Chopra, A.K., October 1980, (PB81 152 324)A11.
- UCB/EERC-80/40 "Inelastic Buckling of Steel Struts under Cyclic Load Reversal," by Black, R.G., Wenger, W.A. and Popov, E.P., October 1980, (PB81 154 312)A08.
- UCB/EERC-80/41 "Influence of Site Characteristics on Buildings Damage during the October 3,1974 Lima Earthquake," by Repetto, P., Arango, I. and Seed, H.B., September 1980, (PB81 161 739)A05.
- UCB/EERC-80/42 "Evaluation of a Shaking Table Test Program on Response Behavior of a Two Story Reinforced Concrete Frame," by Blondet, J.M., Clough, R.W. and Mahin, S.A., December 1980, (PB82 196 544)A11.
- UCB/EERC-80/43 "Modelling of Soil-Structure Interaction by Finite and Infinite Elements," by Medina, F., December 1980, (PB81 229 270)A04.
- UCB/EERC-81/01 "Control of Seismic Response of Piping Systems and Other Structures by Base Isolation," by Kelly, J.M., January 1981, (PB81 200 735)A05.
- UCB/EERC-81/02 "OPTNSR- An Interactive Software System for Optimal Design of Statically and Dynamically Loaded Structures with Nonlinear Response," by Bhatti, M.A., Ciampi, V. and Pister, K.S., January 1981, (PB81 218 851)A09.
- UCB/EERC-81/03 "Analysis of Local Variations in Free Field Seismic Ground Motions," by Chen, J.-C., Lysmer, J. and Seed, H.B., January 1981, (AD-A099508)A13.
- UCB/EERC-81/04 "Inelastic Structural Modeling of Braced Offshore Platforms for Seismic Loading," by Zayas, V.A., Shing, P.-S.B., Mahin, S.A. and Popov, E.P., January 1981, (PB82 138 777)A07.
- UCB/EERC-81/05 "Dynamic Response of Light Equipment in Structures," by Der Kiureghian, A., Sackman, J.L. and Nour-Omid, B., April 1981, (PB81 218 497)A04.
- UCB/EERC-81/06 "Preliminary Experimental Investigation of a Broad Base Liquid Storage Tank," by Bouwkamp, J.G., Kollegger, J.P. and Stephen, R.M., May 1981, (PB82 140 385)A03.
- UCB/EERC-81/07 "The Seismic Resistant Design of Reinforced Concrete Coupled Structural Walls," by Aktan, A.E. and Bertero, V.V., June 1981, (PB82 113 358)A11.
- UCB/EERC-81/08 "Unassigned," by Unassigned, 1981.
- UCB/EERC-81/09 "Experimental Behavior of a Spatial Piping System with Steel Energy Absorbers Subjected to a Simulated Differential Seismic Input," by Stierner, S.F., Godden, W.G. and Kelly, J.M., July 1981, (PB82 201 898)A04.
- UCB/EERC-81/10 "Evaluation of Seismic Design Provisions for Masonry in the United States," by Sveinsson, B.I., Mayes, R.L. and McNiven, H.D., August 1981, (PB82 166 075)A08.
- UCB/EERC-81/11 "Two-Dimensional Hybrid Modelling of Soil-Structure Interaction," by Tzong, T.-J., Gupta, S. and Penzien, J., August 1981, (PB82 142 118)A04.
- UCB/EERC-81/12 "Studies on Effects of Infills in Seismic Resistant R/C Construction," by Brokken, S. and Bertero, V.V., October 1981, (PB82 166 190)A09.
- UCB/EERC-81/13 "Linear Models to Predict the Nonlinear Seismic Behavior of a One-Story Steel Frame," by Valdimarsson, H., Shah, A.H. and McNiven, H.D., September 1981, (PB82 138 793)A07.
- UCB/EERC-81/14 "TLUSH: A Computer Program for the Three-Dimensional Dynamic Analysis of Earth Dams," by Kagawa, T., Mejia, L.H., Seed, H.B. and Lysmer, J., September 1981, (PB82 139 940)A06.
- UCB/EERC-81/15 "Three Dimensional Dynamic Response Analysis of Earth Dams," by Mejia, L.H. and Seed, H.B., September 1981, (PB82 137 274)A12.
- UCB/EERC-81/16 "Experimental Study of Lead and Elastomeric Dampers for Base Isolation Systems," by Kelly, J.M. and Hodder, S.B., October 1981, (PB82 166 182)A05.
- UCB/EERC-81/17 "The Influence of Base Isolation on the Seismic Response of Light Secondary Equipment," by Kelly, J.M., April 1981, (PB82 255 266)A04.
- UCB/EERC-81/18 "Studies on Evaluation of Shaking Table Response Analysis Procedures," by Blondet, J. M., November 1981, (PB82 197 278)A10.
- UCB/EERC-81/19 "DELIGHT.STRUCT: A Computer-Aided Design Environment for Structural Engineering," by Balling, R.J., Pister, K.S. and Polak, E., December 1981, (PB82 218 496)A07.
- UCB/EERC-81/20 "Optimal Design of Seismic-Resistant Planar Steel Frames," by Balling, R.J., Ciampi, V. and Pister, K.S., December 1981, (PB82 220 179)A07.
- UCB/EERC-82/01 "Dynamic Behavior of Ground for Seismic Analysis of Lifeline Systems," by Sato, T. and Der Kiureghian, A., January 1982, (PB82 218 926)A05.
- UCB/EERC-82/02 "Shaking Table Tests of a Tubular Steel Frame Model," by Ghanaat, Y. and Clough, R.W., January 1982, (PB82 220 161)A07.

- UCB/EERC-82/03 "Behavior of a Piping System under Seismic Excitation: Experimental Investigations of a Spatial Piping System supported by Mechanical Shock Arrestors," by Schneider, S., Lee, H.-M. and Godden, W. G., May 1982, (PB83 172 544)A09.
- UCB/EERC-82/04 "New Approaches for the Dynamic Analysis of Large Structural Systems," by Wilson, E.L., June 1982, (PB83 148 080)A05.
- UCB/EERC-82/05 "Model Study of Effects of Damage on the Vibration Properties of Steel Offshore Platforms," by Shahrivar, F. and Bouwkamp, J.G., June 1982, (PB83 148 742)A10.
- UCB/EERC-82/06 "States of the Art and Practice in the Optimum Seismic Design and Analytical Response Prediction of R/C Frame Wall Structures," by Aktan, A.E. and Bertero, V.V., July 1982, (PB83 147 736)A05.
- UCB/EERC-82/07 "Further Study of the Earthquake Response of a Broad Cylindrical Liquid-Storage Tank Model," by Manos, G.C. and Clough, R.W., July 1982, (PB83 147 744)A11.
- UCB/EERC-82/08 "An Evaluation of the Design and Analytical Seismic Response of a Seven Story Reinforced Concrete Frame," by Charney, F.A. and Bertero, V.V., July 1982, (PB83 157 628)A09.
- UCB/EERC-82/09 "Fluid-Structure Interactions: Added Mass Computations for Incompressible Fluid," by Kuo, J.S.-H., August 1982, (PB83 156 281)A07.
- UCB/EERC-82/10 "Joint-Opening Nonlinear Mechanism: Interface Smeared Crack Model," by Kuo, J.S.-H., August 1982, (PB83 149 195)A05.
- UCB/EERC-82/11 "Dynamic Response Analysis of Tchi Dam," by Clough, R.W., Stephen, R.M. and Kuo, J.S.-H., August 1982, (PB83 147 496)A06.
- UCB/EERC-82/12 "Prediction of the Seismic Response of R/C Frame-Coupled Wall Structures," by Aktan, A.E., Bertero, V.V. and Piazzo, M., August 1982, (PB83 149 203)A09.
- UCB/EERC-82/13 "Preliminary Report on the Smart 1 Strong Motion Array in Taiwan," by Bolt, B.A., Loh, C.H., Penzien, J. and Tsai, Y.B., August 1982, (PB83 159 400)A10.
- UCB/EERC-82/14 "Shaking-Table Studies of an Eccentrically X-Braced Steel Structure," by Yang, M.S., September 1982, (PB83 260 778)A12.
- UCB/EERC-82/15 "The Performance of Stairways in Earthquakes," by Roha, C., Axley, J.W. and Bertero, V.V., September 1982, (PB83 157 693)A07.
- UCB/EERC-82/16 "The Behavior of Submerged Multiple Bodies in Earthquakes," by Liao, W.-G., September 1982, (PB83 158 709)A07.
- UCB/EERC-82/17 "Effects of Concrete Types and Loading Conditions on Local Bond-Slip Relationships," by Cowell, A.D., Popov, E.P. and Bertero, V.V., September 1982, (PB83 153 577)A04.
- UCB/EERC-82/18 "Mechanical Behavior of Shear Wall Vertical Boundary Members: An Experimental Investigation," by Wagner, M.T. and Bertero, V.V., October 1982, (PB83 159 764)A05.
- UCB/EERC-82/19 "Experimental Studies of Multi-support Seismic Loading on Piping Systems," by Kelly, J.M. and Cowell, A.D., November 1982.
- UCB/EERC-82/20 "Generalized Plastic Hinge Concepts for 3D Beam-Column Elements," by Chen, P. F.-S. and Powell, G.H., November 1982, (PB83 247 981)A13.
- UCB/EERC-82/21 "ANSR-II: General Computer Program for Nonlinear Structural Analysis," by Oughourlian, C.V. and Powell, G.H., November 1982, (PB83 251 330)A12.
- UCB/EERC-82/22 "Solution Strategies for Statically Loaded Nonlinear Structures," by Simons, J.W. and Powell, G.H., November 1982, (PB83 197 970)A06.
- UCB/EERC-82/23 "Analytical Model of Deformed Bar Anchorages under Generalized Excitations," by Ciampi, V., Eligehausen, R., Bertero, V.V. and Popov, E.P., November 1982, (PB83 169 532)A06.
- UCB/EERC-82/24 "A Mathematical Model for the Response of Masonry Walls to Dynamic Excitations," by Sucuoglu, H., Mengi, Y. and McNiven, H.D., November 1982, (PB83 169 011)A07.
- UCB/EERC-82/25 "Earthquake Response Considerations of Broad Liquid Storage Tanks," by Cambra, F.J., November 1982, (PB83 251 215)A09.
- UCB/EERC-82/26 "Computational Models for Cyclic Plasticity, Rate Dependence and Creep," by Mosaddad, B. and Powell, G.H., November 1982, (PB83 245 829)A08.
- UCB/EERC-82/27 "Inelastic Analysis of Piping and Tubular Structures," by Mahasuverachai, M. and Powell, G.H., November 1982, (PB83 249 987)A07.
- UCB/EERC-83/01 "The Economic Feasibility of Seismic Rehabilitation of Buildings by Base Isolation," by Kelly, J.M., January 1983, (PB83 197 988)A05.
- UCB/EERC-83/02 "Seismic Moment Connections for Moment-Resisting Steel Frames," by Popov, E.P., January 1983, (PB83 195 412)A04.
- UCB/EERC-83/03 "Design of Links and Beam-to-Column Connections for Eccentrically Braced Steel Frames," by Popov, E.P. and Malley, J.O., January 1983, (PB83 194 811)A04.
- UCB/EERC-83/04 "Numerical Techniques for the Evaluation of Soil-Structure Interaction Effects in the Time Domain," by Bayo, E. and Wilson, E.L., February 1983, (PB83 245 605)A09.
- UCB/EERC-83/05 "A Transducer for Measuring the Internal Forces in the Columns of a Frame-Wall Reinforced Concrete Structure," by Sause, R. and Bertero, V.V., May 1983, (PB84 119 494)A06.
- UCB/EERC-83/06 "Dynamic Interactions Between Floating Ice and Offshore Structures," by Croteau, P., May 1983, (PB84 119 486)A16.
- UCB/EERC-83/07 "Dynamic Analysis of Multiply Tuned and Arbitrarily Supported Secondary Systems," by Igusa, T. and Der Kiureghian, A., July 1983, (PB84 118 272)A11.
- UCB/EERC-83/08 "A Laboratory Study of Submerged Multi-body Systems in Earthquakes," by Ansari, G.R., June 1983, (PB83 261 842)A17.
- UCB/EERC-83/09 "Effects of Transient Foundation Uplift on Earthquake Response of Structures," by Yim, C.-S. and Chopra, A.K., June 1983, (PB83 261 396)A07.
- UCB/EERC-83/10 "Optimal Design of Friction-Braced Frames under Seismic Loading," by Austin, M.A. and Pister, K.S., June 1983, (PB84 119 288)A06.
- UCB/EERC-83/11 "Shaking Table Study of Single-Story Masonry Houses: Dynamic Performance under Three Component Seismic Input and Recommendations," by Manos, G.C., Clough, R.W. and Mayes, R.L., July 1983, (UCB/EERC-83/11)A08.
- UCB/EERC-83/12 "Experimental Error Propagation in Pseudodynamic Testing," by Shiing, P.B. and Mahin, S.A., June 1983, (PB84 119 270)A09.
- UCB/EERC-83/13 "Experimental and Analytical Predictions of the Mechanical Characteristics of a 1/5-scale Model of a 7-story R/C Frame-Wall Building Structure," by Aktan, A.E., Bertero, V.V., Chowdhury, A.A. and Nagashima, T., June 1983, (PB84 119 213)A07.

- UCB/EERC-83/14 "Shaking Table Tests of Large-Panel Precast Concrete Building System Assemblages," by Oliva, M.G. and Clough, R.W., June 1983, (PB86 110 210/AS)A11.
- UCB/EERC-83/15 "Seismic Behavior of Active Beam Links in Eccentrically Braced Frames," by Hjelmstad, K.D. and Popov, E.P., July 1983, (PB84 119 676)A09.
- UCB/EERC-83/16 "System Identification of Structures with Joint Rotation," by Dimsdale, J.S., July 1983, (PB84 192 210)A06.
- UCB/EERC-83/17 "Construction of Inelastic Response Spectra for Single-Degree-of-Freedom Systems," by Mahin, S. and Lin, J., June 1983, (PB84 208 834)A05.
- UCB/EERC-83/18 "Interactive Computer Analysis Methods for Predicting the Inelastic Cyclic Behaviour of Structural Sections," by Kaba, S. and Mahin, S., July 1983, (PB84 192 012)A06.
- UCB/EERC-83/19 "Effects of Bond Deterioration on Hysteretic Behavior of Reinforced Concrete Joints," by Filippou, F.C., Popov, E.P. and Bertero, V.V., August 1983, (PB84 192 020)A10.
- UCB/EERC-83/20 "Analytical and Experimental Correlation of Large-Panel Precast Building System Performance," by Oliva, M.G., Clough, R.W., Velkov, M. and Gavrilovic, P., November 1983.
- UCB/EERC-83/21 "Mechanical Characteristics of Materials Used in a 1/5 Scale Model of a 7-Story Reinforced Concrete Test Structure," by Bertero, V.V., Aktan, A.E., Harris, H.G. and Chowdhury, A.A., October 1983, (PB84 193 697)A05.
- UCB/EERC-83/22 "Hybrid Modelling of Soil-Structure Interaction in Layered Media," by Tzong, T.-J. and Penzien, J., October 1983, (PB84 192 178)A08.
- UCB/EERC-83/23 "Local Bond Stress-Slip Relationships of Deformed Bars under Generalized Excitations," by Eligehausen, R., Popov, E.P. and Bertero, V.V., October 1983, (PB84 192 848)A09.
- UCB/EERC-83/24 "Design Considerations for Shear Links in Eccentrically Braced Frames," by Malley, J.O. and Popov, E.P., November 1983, (PB84 192 186)A07.
- UCB/EERC-84/01 "Pseudodynamic Test Method for Seismic Performance Evaluation: Theory and Implementation," by Shing, P.-S.B. and Mahin, S.A., January 1984, (PB84 190 644)A08.
- UCB/EERC-84/02 "Dynamic Response Behavior of Kiang Hong Dian Dam," by Clough, R.W., Chang, K.-T., Chen, H.-Q. and Stephen, R.M., April 1984, (PB84 209 402)A08.
- UCB/EERC-84/03 "Refined Modelling of Reinforced Concrete Columns for Seismic Analysis," by Kaba, S.A. and Mahin, S.A., April 1984, (PB84 234 384)A06.
- UCB/EERC-84/04 "A New Floor Response Spectrum Method for Seismic Analysis of Multiply Supported Secondary Systems," by Asfura, A. and Der Kiureghian, A., June 1984, (PB84 239 417)A06.
- UCB/EERC-84/05 "Earthquake Simulation Tests and Associated Studies of a 1/5th-scale Model of a 7-Story R/C Frame-Wall Test Structure," by Bertero, V.V., Aktan, A.E., Charney, F.A. and Sause, R., June 1984, (PB84 239 409)A09.
- UCB/EERC-84/06 "R/C Structural Walls: Seismic Design for Shear," by Aktan, A.E. and Bertero, V.V., 1984.
- UCB/EERC-84/07 "Behavior of Interior and Exterior Flat-Plate Connections subjected to Inelastic Load Reversals," by Zee, H.L. and Mochle, J.P., August 1984, (PB86 117 629/AS)A07.
- UCB/EERC-84/08 "Experimental Study of the Seismic Behavior of a Two-Story Flat-Plate Structure," by Mochle, J.P. and Diebold, J.W., August 1984, (PB86 122 553/AS)A12.
- UCB/EERC-84/09 "Phenomenological Modeling of Steel Braces under Cyclic Loading," by Ikeda, K., Mahin, S.A. and Dermitzakis, S.N., May 1984, (PB86 132 198/AS)A08.
- UCB/EERC-84/10 "Earthquake Analysis and Response of Concrete Gravity Dams," by Fenves, G. and Chopra, A.K., August 1984, (PB85 193 902/AS)A11.
- UCB/EERC-84/11 "EAGD-84: A Computer Program for Earthquake Analysis of Concrete Gravity Dams," by Fenves, G. and Chopra, A.K., August 1984, (PB85 193 613/AS)A05.
- UCB/EERC-84/12 "A Refined Physical Theory Model for Predicting the Seismic Behavior of Braced Steel Frames," by Ikeda, K. and Mahin, S.A., July 1984, (PB85 191 450/AS)A09.
- UCB/EERC-84/13 "Earthquake Engineering Research at Berkeley - 1984," by , August 1984, (PB85 197 341/AS)A10.
- UCB/EERC-84/14 "Moduli and Damping Factors for Dynamic Analyses of Cohesionless Soils," by Seed, H.B., Wong, R.T., Idriss, I.M. and Tokimatsu, K., September 1984, (PB85 191 468/AS)A04.
- UCB/EERC-84/15 "The Influence of SPT Procedures in Soil Liquefaction Resistance Evaluations," by Seed, H.B., Tokimatsu, K., Harder, L.F. and Chung, R.M., October 1984, (PB85 191 732/AS)A04.
- UCB/EERC-84/16 "Simplified Procedures for the Evaluation of Settlements in Sands Due to Earthquake Shaking," by Tokimatsu, K. and Seed, H.B., October 1984, (PB85 197 887/AS)A03.
- UCB/EERC-84/17 "Evaluation of Energy Absorption Characteristics of Bridges under Seismic Conditions," by Imbsen, R.A. and Penzien, J., November 1984.
- UCB/EERC-84/18 "Structure-Foundation Interactions under Dynamic Loads," by Liu, W.D. and Penzien, J., November 1984, (PB87 124 889/AS)A11.
- UCB/EERC-84/19 "Seismic Modelling of Deep Foundations," by Chen, C.-H. and Penzien, J., November 1984, (PB87 124 798/AS)A07.
- UCB/EERC-84/20 "Dynamic Response Behavior of Quan Shui Dam," by Clough, R.W., Chang, K.-T., Chen, H.-Q., Stephen, R.M., Ghanaat, Y. and Qi, J.-H., November 1984, (PB86 115177/AS)A07.
- UCB/EERC-85/01 "Simplified Methods of Analysis for Earthquake Resistant Design of Buildings," by Cruz, E.F. and Chopra, A.K., February 1985, (PB86 112299/AS)A12.
- UCB/EERC-85/02 "Estimation of Seismic Wave Coherency and Rupture Velocity using the SMART 1 Strong-Motion Array Recordings," by Abrahamson, N.A., March 1985, (PB86 214 343)A07.

- UCB/EERC-85/03 "Dynamic Properties of a Thirty Story Condominium Tower Building," by Stephen, R.M., Wilson, E.L. and Stander, N., April 1985, (PB86 118965/AS)A06.
- UCB/EERC-85/04 "Development of Substructuring Techniques for On-Line Computer Controlled Seismic Performance Testing," by Dermitzakis, S. and Mahin, S., February 1985, (PB86 132941/AS)A08.
- UCB/EERC-85/05 "A Simple Model for Reinforcing Bar Anchorages under Cyclic Excitations," by Filippou, F.C., March 1985, (PB86 112 919/AS)A05.
- UCB/EERC-85/06 "Racking Behavior of Wood-framed Gypsum Panels under Dynamic Load," by Oliva, M.G., June 1985.
- UCB/EERC-85/07 "Earthquake Analysis and Response of Concrete Arch Dams," by Fok, K.-L. and Chopra, A.K., June 1985, (PB86 139672/AS)A10.
- UCB/EERC-85/08 "Effect of Inelastic Behavior on the Analysis and Design of Earthquake Resistant Structures," by Lin, J.P. and Mahin, S.A., June 1985, (PB86 135340/AS)A08.
- UCB/EERC-85/09 "Earthquake Simulator Testing of a Base-Isolated Bridge Deck," by Kelly, J.M., Buckle, I.G. and Tsai, H.-C., January 1986, (PB87 124 152/AS)A06.
- UCB/EERC-85/10 "Simplified Analysis for Earthquake Resistant Design of Concrete Gravity Dams," by Fenves, G. and Chopra, A.K., June 1986, (PB87 124 160/AS)A08.
- UCB/EERC-85/11 "Dynamic Interaction Effects in Arch Dams," by Clough, R.W., Chang, K.-T., Chen, H.-Q. and Ghanaat, Y., October 1985, (PB86 135027/AS)A05.
- UCB/EERC-85/12 "Dynamic Response of Long Valley Dam in the Mammoth Lake Earthquake Series of May 25-27, 1980," by Lai, S. and Seed, H.B., November 1985, (PB86 142304/AS)A05.
- UCB/EERC-85/13 "A Methodology for Computer-Aided Design of Earthquake-Resistant Steel Structures," by Austin, M.A., Pister, K.S. and Mahin, S.A., December 1985, (PB86 159480/AS)A10.
- UCB/EERC-85/14 "Response of Tension-Leg Platforms to Vertical Seismic Excitations," by Liou, G.-S., Penzien, J. and Yeung, R.W., December 1985, (PB87 124 871/AS)A08.
- UCB/EERC-85/15 "Cyclic Loading Tests of Masonry Single Piers: Volume 4 - Additional Tests with Height to Width Ratio of 1," by Sveinsson, B., McNiven, H.D. and Sucuoglu, H., December 1985.
- UCB/EERC-85/16 "An Experimental Program for Studying the Dynamic Response of a Steel Frame with a Variety of Infill Partitions," by Yanev, B. and McNiven, H.D., December 1985.
- UCB/EERC-86/01 "A Study of Seismically Resistant Eccentrically Braced Steel Frame Systems," by Kasai, K. and Popov, E.P., January 1986, (PB87 124 178/AS)A14.
- UCB/EERC-86/02 "Design Problems in Soil Liquefaction," by Seed, H.B., February 1986, (PB87 124 186/AS)A03.
- UCB/EERC-86/03 "Implications of Recent Earthquakes and Research on Earthquake-Resistant Design and Construction of Buildings," by Bertero, V.V., March 1986, (PB87 124 194/AS)A05.
- UCB/EERC-86/04 "The Use of Load Dependent Vectors for Dynamic and Earthquake Analyses," by Leger, P., Wilson, E.L. and Clough, R.W., March 1986, (PB87 124 202/AS)A12.
- UCB/EERC-86/05 "Two Beam-To-Column Web Connections," by Tsai, K.-C. and Popov, E.P., April 1986, (PB87 124 301/AS)A04.
- UCB/EERC-86/06 "Determination of Penetration Resistance for Coarse-Grained Soils using the Becker Hammer Drill," by Harder, L.F. and Seed, H.B., May 1986, (PB87 124 210/AS)A07.
- UCB/EERC-86/07 "A Mathematical Model for Predicting the Nonlinear Response of Unreinforced Masonry Walls to In-Plane Earthquake Excitations," by Mengi, Y. and McNiven, H.D., May 1986, (PB87 124 780/AS)A06.
- UCB/EERC-86/08 "The 19 September 1985 Mexico Earthquake: Building Behavior," by Bertero, V.V., July 1986.
- UCB/EERC-86/09 "EACD-3D: A Computer Program for Three-Dimensional Earthquake Analysis of Concrete Dams," by Fok, K.-L., Hall, J.F. and Chopra, A.K., July 1986, (PB87 124 228/AS)A08.
- UCB/EERC-86/10 "Earthquake Simulation Tests and Associated Studies of a 0.3-Scale Model of a Six-Story Concentrically Braced Steel Structure," by Uang, C.-M. and Bertero, V.V., December 1986, (PB87 163 564/AS)A17.
- UCB/EERC-86/11 "Mechanical Characteristics of Base Isolation Bearings for a Bridge Deck Model Test," by Kelly, J.M., Buckle, I.G. and Koh, C.-G., 1987.
- UCB/EERC-86/12 "Effects of Axial Load on Elastomeric Isolation Bearings," by Koh, C.-G. and Kelly, J.M., 1987.
- UCB/EERC-87/01 "The FPS Earthquake Resisting System: Experimental Report," by Zayas, V.A., Low, S.S. and Mahin, S.A., June 1987.
- UCB/EERC-87/02 "Earthquake Simulator Tests and Associated Studies of a 0.3-Scale Model of a Six-Story Eccentrically Braced Steel Structure," by Whittaker, A., Uang, C.-M. and Bertero, V.V., July 1987.
- UCB/EERC-87/03 "A Displacement Control and Uplift Restraint Device for Base-Isolated Structures," by Kelly, J.M., Griffith, M.C. and Aiken, LD., April 1987.
- UCB/EERC-87/04 "Earthquake Simulator Testing of a Combined Sliding Bearing and Rubber Bearing Isolation System," by Kelly, J.M. and Chalhoub, M.S., 1987.
- UCB/EERC-87/05 "Three-Dimensional Inelastic Analysis of Reinforced Concrete Frame-Wall Structures," by Moazzami, S. and Bertero, V.V., May 1987.
- UCB/EERC-87/06 "Experiments on Eccentrically Braced Frames with Composite Floors," by Ricles, J. and Popov, E., June 1987.
- UCB/EERC-87/07 "Dynamic Analysis of Seismically Resistant Eccentrically Braced Frames," by Ricles, J. and Popov, E., June 1987.
- UCB/EERC-87/08 "Undrained Cyclic Triaxial Testing of Gravels-The Effect of Membrane Compliance," by Evans, M.D. and Seed, H.B., July 1987.
- UCB/EERC-87/09 "Hybrid Solution Techniques for Generalized Pseudo-Dynamic Testing," by Thewalt, C. and Mahin, S.A., July 1987.
- UCB/EERC-87/10 "Ultimate Behavior of Butt Welded Splices in Heavy Rolled Steel Sections," by Bruneau, M. Mahin, S.A. and Popov, E., September 1987.
- UCB/EERC-87/11 "Residual Strength of Sand from Dam Failures in the Chilean Earthquake of March 3, 1985," by De Alba, P., Seed, H.B., Retamal, E. and Seed, R.B., September 1987.

- UCB/EERC-87/12 "Inelastic Seismic Response of Structures with Mass or Stiffness Eccentricities in Plan," by Bruncau, M. and Mahin, S.A., September 1987.
- UCB/EERC-87/13 "CSTRUCT: An Interactive Computer Environment for the Design and Analysis of Earthquake Resistant Steel Structures," by Austin, M.A., Mahin, S.A. and Pister, K.S., September 1987.
- UCB/EERC-87/14 "Experimental Study of Reinforced Concrete Columns Subjected to Multi-Axial Loading," by Low, S.S. and Moehle, J.P., September 1987.
- UCB/EERC-87/15 "Relationships between Soil Conditions and Earthquake Ground Motions in Mexico City in the Earthquake of Sept. 19, 1985," by Seed, H.B., Romo, M.P., Sun, J., Jaime, A. and Lysmer, J., October 1987.
- UCB/EERC-87/16 "Experimental Study of Seismic Response of R. C. Setback Buildings," by Shahrooz, B.M. and Moehle, J.P., October 1987.
- UCB/EERC-87/17 "The Effect of Slabs on the Flexural Behavior of Beams," by Pantazopoulou, S.J. and Moehle, J.P., October 1987.
- UCB/EERC-87/18 "Design Procedure for R-FBI Bearings," by Mostaghel, N. and Kelly, J.M., November 1987.
- UCB/EERC-87/19 "Analytical Models for Predicting the Lateral Response of R C Shear Walls: Evaluation of their Reliability," by Vulcano, A. and Bertero, V.V., November 1987.
- UCB/EERC-87/20 "Earthquake Response of Torsionally-Coupled Buildings," by Hejal, R. and Chopra, A.K., December 1987.
- UCB/EERC-87/21 "Dynamic Reservoir Interaction with Monticello Dam," by Clough, R.W., Ghanaat, Y. and Qiu, X-F., December 1987.
- UCB/EERC-87/22 "Strength Evaluation of Coarse-Grained Soils," by Siddiqi, F.H., Seed, R.B., Chan, C.K., Seed, H.B. and Pyke, R.M., December 1987.
- UCB/EERC-88/01 "Seismic Behavior of Concentrically Braced Steel Frames," by Khatib, I., Mahin, S.A. and Pister, K.S., January 1988.
- UCB/EERC-88/02 "Experimental Evaluation of Seismic Isolation of Medium-Rise Structures Subject to Uplift," by Griffith, M.C., Kelly, J.M., Coveney, V.A. and Koh, C.G., January 1988.
- UCB/EERC-88/03 "Cyclic Behavior of Steel Double Angle Connections," by Astaneh-Asl, A. and Nader, M.N., January 1988.
- UCB/EERC-88/04 "Re-evaluation of the Slide in the Lower San Fernando Dam in the Earthquake of Feb. 9, 1971," by Seed, H.B., Seed, R.B., Harder, L.F. and Jong, H.-L., April 1988.
- UCB/EERC-88/05 "Experimental Evaluation of Seismic Isolation of a Nine-Story Braced Steel Frame Subject to Uplift," by Griffith, M.C., Kelly, J.M. and Aiken, I.D., May 1988.
- UCB/EERC-88/06 "DRAIN-2DX User Guide," by Allahabadi, R. and Powell, G.H., March 1988.
- UCB/EERC-88/07 "Cylindrical Fluid Containers in Base-Isolated Structures," by Chalhoub, M.S. and Kelly, J.M., April 1988.
- UCB/EERC-88/08 "Analysis of Near-Source Waves: Separation of Wave Types using Strong Motion Array Recordings," by Darragh, R.B., June 1988.
- UCB/EERC-88/09 "Alternatives to Standard Mode Superposition for Analysis of Non-Classically Damped Systems," by Kusainov, A.A. and Clough, R.W., June 1988.
- UCB/EERC-88/10 "The Landslide at the Port of Nice on October 16, 1979," by Seed, H.B., Seed, R.B., Schlosser, F., Blondeau, F. and Juran, I., June 1988.
- UCB/EERC-88/11 "Liquefaction Potential of Sand Deposits Under Low Levels of Excitation," by Carter, D.P. and Seed, H.B., August 1988.
- UCB/EERC-88/12 "Analysis of Nonlinear Response of Reinforced Concrete Frames to Cyclic Load Reversals," by Filippou, F.C. and Issa, A., September 1988.
- UCB/EERC-88/13 "Earthquake-Resistant Design of Building Structures: An Energy Approach," by Uang, C.-M. and Bertero, V.V., September 1988.
- UCB/EERC-88/14 "An Experimental Study of the Behavior of Dual Steel Systems," by Whittaker, A.S., Uang, C.-M. and Bertero, V.V., September 1988.
- UCB/EERC-88/15 "Dynamic Moduli and Damping Ratios for Cohesive Soils," by Sun, J.I., Golesorkhi, R. and Seed, H.B., August 1988.
- UCB/EERC-88/16 "Reinforced Concrete Flat Plates Under Lateral Load: An Experimental Study Including Biaxial Effects," by Pan, A. and Moehle, J., November 1988.
- UCB/EERC-88/17 "Earthquake Engineering Research at Berkeley - 1988," November 1988.
- UCB/EERC-88/18 "Use of Energy as a Design Criterion in Earthquake-Resistant Design," by Uang, C.-M. and Bertero, V.V., November 1988.